NANOSTRUCTURES AND PATTERNING IN INDIAN PARROT *Psittacula krameri.*

A THESIS SUBMITTED IN FULFILLMENT OFTHE DEGREE OF

Master In Life Science

By
PRIYADARSHANI SUCHISMITA SETHY
413LS2050

Under The Supervision of

Dr. MONALISA MISRA

DEPARTMENT OF LIFE SCIENCE
NATIONAL INSTITUTE OF TECHNOLOGY
ROURKELA-769008, ORISSA,2015

CERTIFICATE

This is to certify that**, Priyadarshani Suchismita Sethy** (Roll number: 413LS2050), a final year student of M.sc (2 years), batch 2013-2015, of this institute, has successfully submitted the project titled "**NANOSTRUCTURES AND PATTERNING IN INDIAN PARROT *Psittacula krameri"*** to **NATIONAL INSTITUTE OF TECHNOLOGY ROURKELA** under my supervision. I believe that the thesis fulfill part of the requirements for the award of Master of Science in LIFE SCINCES. The results embodied in the thesis have not been submitted for the award of any other degree.

Dr .MONALISA MISHRA
Associate Professor
Department of Life Science
National Institute of Technology, Rourkela, Orissa,India

DECLARATION

I hereby declare that the thesis entitled "**NANOSTRUCTURES AND PATTERNING IN INDIAN PARROT *Psittacula krameri.*"** submitted to Department of Life Science, National Institute of Technology, Rourkela for the partial fulfillment of the requirements for the degree of master of science in life science is an original piece of research work done by me under the guidance of Dr. Monalisa Mishra, Assistant Professor, Department of Life Science, National Institute of Technology, Rourkela. No part of this work has been done by any other research person and has not been submitted for any other purpose.

PRIYADARSHANI SUCHISMITA SETHY

413LS2050

ACKNOWLEDGEMENT

I take the privilege to express my utmost gratitude to my guide Dr. Monalisa Mishra, Assistant Professor, Department of Life Science, National Institute of Technology, Rourkela for her idea, excellent guidance, care, patience and for providing me with every facility to complete my dissertation.

I am thankful to National Institute of Technology, Rourkela, for providing all equipment I required in the course of this project in order to complete it.

I convey my deepest gratitude to Mr. Debabrat Sabat (PhD Scholar), Department of Life Science, National Institute of Technology, Rourkela, for his care, co-operation, patience and timely advice in each and every step of my work.

I would also like to thank all my classmates and my lab mates for their help and support during my work. Last but not the least, I express my heartiest devotion to my beloved parents for their ethical and moral support, love and blessings which helped in the successful completion of my dissertation.

I bow my head before the Almighty for his blessings on me.

CONTENTS

LIST OF FIGURES

ABBREVIATIONS

XRD: X-ray diffraction

UV: Ultra violet

SEM: Scanning Electron Microscope

NPS: Nanoparticles

ROS: Reactive Oxygen Species

NM: Nanomedicines

µM: Micrometer

nm: nanometer

ABSTRACT:

The Indian parakeet (*Psittacula krameri)* belongs to the order *Psittaciformes* family *Psittacidae*. The male has a red ring in the neck collar region hence called rose ringed parakeet while the female lack it, showing sexual dimorphism. Parrots attract because of their phenomenal feather coloration which is because of iridescent and non-iridescent phenomenon of light. They show different color when they are viewed from different angle and the phenomena is called iridescent. It has been reported that the coloration is due to the microstructures that are present in barb. To some extend these microstructures are responsible for UV reflectance property of these feathers. It has been reported that the coloration is also due to nanostructures present on parrot's feather and as well as the structure and pattern formation of different feather components of parrot. Here the XRD analyses of the feathers were done and the elements were detected using the EDX software, and some of their possible functions were predicted. Apart from this UV reflectance of various feathers were examined, where some show UV reflectance and some lack it. The possible function of UV reflectance is predicted to be useful in mate selection. Most importantly to understand pattern formation of various feather components the SEM was used.

Key words: Parakeet, Scanning electron microscopy (SEM), X-ray diffraction (XRD), Nanoparticles (NP), Nanomedicines (NM), Iridescent, UV reflectance.

INTRODUCTION:

Birds captivated us the eternal not only because of their flight but also the diverse color they exhibit to make world colorful. The coloration of bird's feathers are due to pigmentation that is carotenoids and melanin(Olson and Owens 1998, Jawor and Breitwisch 2003)and also due to microstructures that are present on barbs (Fox 1976, Prum, Andersson et al. 2003). These microstructures are responsible for production of blue, violet, iridescent colors and ultraviolet (UV) which cannot be detected by human eye. UV reflective feathers are wide spread in many bird species (Burkhardt 1989, Eaton and Lanyon 2003, Hausmann, Arnold et al. 2003) and many birds have the ability to see in the UV region of spectrum(Parrish, Ptacek et al. 1984, Cuthill, Partridge et al. 2000).

Carotenoids responsible for production of bright red to orange and yellow coloration and achromatic brown or black coloration are attributed by melanin(Fox 1976, Olson and Owens 1998). Carotenoids cannot be synthesized by the vertebrates so they only can be derived from food and modified later for its color attribution to the feathers (Brush 1990, Hill 2000). It has been proposed that carotenoids may be used as a signal by the females to identify potential male (Hill, Inouye et al. 2002, Faivre, Grégoire et al. 2003, Grether, Kolluru et al. 2005).Carotenoids must be absorbed transported and deposited to give feather coloration and this phenomenon may require energy(Hill, Inouye et al. 2002, Hill and McGraw 2006).Carotenoid based coloration may confer information on the nutritional, parasitic and general body condition of the bearer (Hill 1999).Melanins are synthesized by the amino acid precursors tyrosine(Jawor and Breitwisch, 2003). Recently it has been reported by some authors that melanin also produces some other colors like chestnut, orange and yellow which are believed to be produce by carotenoids including the orange cheeks of the zebra finch *Taeniopygiaguttata* (McGraw et al., 2003a), the chestnut of European and American barn [i]swallows *Hirundorustica* and *H. erythrogaster* (McGraw, Safran et al. 2004), and the yellow portion of red-winged blackbird *Agelaiusphoeniceus*. These bright colors are produced by phaeomelanins rather than eumelanins(M Hofmann, J McGraw et al. 2007). The color is produced by the light absorbed by the pigment.

Another factor of coloration in birds are due to structural coloration. Structural colors include the blue, violet, ultraviolet and iridescent patches of feathers and skin (Auber 1957, DYCK

1985).This structural coloration occur due to scattering of coherent light by the nanostructure arrangement of the various feather components like keratin melanin and air in barbs and barbules. The structural coloration produce due to refractive index variation of all those feathers (Prum 2006). However it has been reported that the structural coloration are due to the melanin containing organelles called melanosomes they are formed during the course of development (Maia, Brasileiro et al. 2012), to form hexagonal closed packed structures (Durrer, 1977). Brighter and more contrasting saturated colors can be produced by increasing the contrast refractive index, increasing the relative amount of elements of low refractive index (keratin) by adding space between melanosomes, with potentially decreasing order (Torquato, Truskett et al. 2000). This pattern of coloration is called iridescent that is different colors are observed when viewed from different angles (Newton) and this phenomena is very common in birds (Yoshioka and Kinoshita 2002, Eliason and Shawkey 2012). Another subtype of structural coloration is non-iridescent. Non-iridescent colors generally remain similar in appearance regardless of viewing geometry or angle of observation (Newton 1952). Barbule curvature influences the orientation of the melanosomes with respect to the viewer which is responsible for the production of structural coloration (Wilts, Michielsen et al. 2012).

However there are some exceptions found in case of parrot. They show a wide variety of coloration that is from red to yellow in their feathers, but they don't derive their coloration from carotenoids (Hudon and Brush 1992). They derive their coloration from a specific class of biochromes called psittacofulvins (Krukenberg 1882). However psittacofulvins show similar characterstics as of the carotenoids like they have similar light reflectance based on their C=C bond (Veronelli, Zerbi et al. 1995), similarity in solubility (Hudon and Brush1992) and follow an equal mechanism to incorporate into feathers for exhibiting color. As they are lipids it is believed that they get into the follicles from blood stream by passive diffusion (Lucas and Stettenheim 1972). The physiological and anatomical origin of psittacofulvins are not known (Stradi, Pini et al. 2001). Why parrots use psittacofulvin instead of carotenoids is an open question. Although parrots have a capability to accumulate carotenoids in a significant amount still they fail to incorporate it into feathers for coloration (McGraw and Nogare 2004). These pigments are also not obtained from diet as the blood shows the absence of psittacofulvins (McGraw and Nogare 2004). Hence like other birds parrots don't show a change in color in the disturbance of nutrition (Nemésio 2001). Their absence in blood also shows that they are synthesized locally but not

centrally (McGraw and Nogare 2004). It is expected that they might be synthesized at the mature follicles of growing feathers (McGraw and Nogare 2004), as melanins are synthesized within the feather tract (Ralph 1969), and carotenoids are synthesized at the feather follicle (Stradi 1998). Parrots may be the only class of aves who synthesize their own pigments (McGraw 2005) and they show composite coloration, both pigmentation and structural coloration.. Here we made a study on the structure, structural arrangement and pattern formation by different feather components of parrot, taken from different parts of its body and there by predicted some of their possible functions. Here we will study regarding the Indian rose ringed parakeet *Psittacula krameri* of Class-Aves, Order-Psittaciformes, Superfamily- Psittacoidea, Family- Psittaculidae, Sub family- Psittaculinae, Tribe- Psittaculini, Genus- *Psittacula*, Species-*Krameri***.**

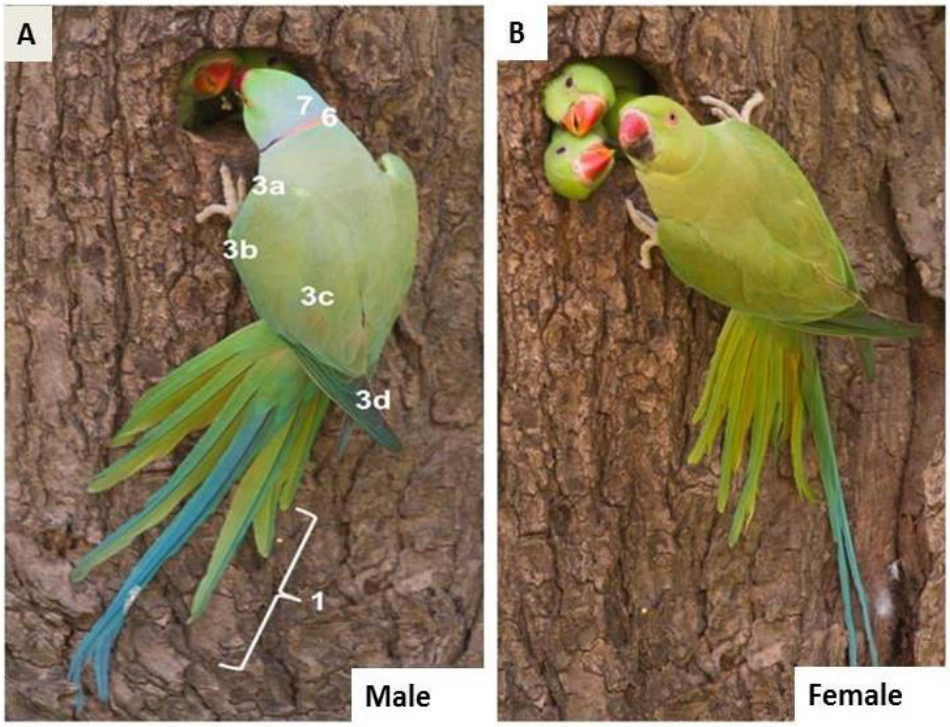

Figure 1: Plumage pattern of the rose-ringed parakeet.

1 – Long graduated tail, 3a – Shoulder or scapulars & lesser coverts, 3b – curved wing feathers, 3c – Leaf-shaped wing feathers, 3d – Flight feathers, 6-Rose (red) colored ring is identification mark of male rose-ringed parakeet, 7- Head feather.

LITERATURE SURVEY:

PRINCIPLE OF XRD:

In order to understand the function of various biological structures it is important to study their structure as well as the structural interactions. Although a number of high resolution microscopes have been developed the only method that currently yields better result of biological structure at atomic level of resolution is X-ray diffraction from a single crystal. This technique involve three distinct steps, i) growing a crystal ii) collecting X-ray diffraction pattern from the crystals iii) constructing and refining a structural model from the crystals to fit the X-ray diffraction pattern. A molecular structure solved to atomic resolution means the position of each atom can be distinguished from those of all atom in three dimensional space without applying any assumptions regarding the structure of molecule. The closest distance between the two atoms in space is the length of covalent bond between them. Since the approximate distance between a covalent bond is 0.12nm we need to see two atoms as distinct particles. There are theoretical and practical limitations to resolve a structure to this fine level. First the system has its atoms of its molecules held rigidly and second each molecule or group of molecules in the system must have identical confirmation. We must now find a radiation source that allows us to see two atoms separated by a radius 0.12nm. The limit of resolution (LR) of any optical method is defined by the wavelength lambda of the incident radiation.

$$LR = \lambda/2$$

This is because an extension of Heisenberg's principle that results from treating light as a wave states that the position of a particle cannot be fixed to better than about half the wavelength of the radiation used to examine that particle. If we require the resolution of the technique to be 0.12nm to resolve the atoms of a molecule, the wavelength of the light required to be 0.24nm. This falls into the X-ray range of electromagnetic spectrum. As x-rays cannot be focused to obtain the image as we get by light microscope, so we have to depend upon the constructive and destructive inference we obtain depending upon the scattering of radiation by the regular and repeating lattice of the crystals to determine the structure. The energy of a quantum of X-ray radiation is equivalent to 8000eV which is approximately equal to the energy of the all electrons present on its orbit. This equivalence of the energy leads to interaction so that the electrons of an

atom are primarily responsible for the scattering of X-rays. The numbers of electrons present in a given volume or space determines how strongly an atom scatters x-rays. The interference of the scattered x-rays leads to the general phenomenon of diffraction.

How x-ray diffraction is used to study the structures:

All electromagnetic radiations have dual nature of matter, both particulate as well as wave nature of matter. In x-ray scattering we treat all electromagnetic radiation as waves. Scattering simply refers to the ability of an object to change the direction of waves. An object placed in the path of a light from a point of source cannot cast a sharp shadow because of scattering from its edges. The origin of scattering of light can be best understood from Huygens's principle that "every point along a wave front can be considered to be the origin of a new wave front. The velocity of this new wave front can be considered to be same as the original one. Objects placed on the path of a wave front act as a point of propagation of new waves. The entirely new wave is called scattered wave. If we place two objects A and B on the path of a wave front each of the two objects will propagate a new wave front having identical wavelength and velocities. At some position in space the wave propagating from point A will reinforce the scattered wave from point B through constructive interference through if the two scattered waves are in phase. If the amplitude of the wave A reduces the amplitude of the wave B then it is said waves are out of phase hence called destructive interference. This is called diffraction, the sum of the two waves propagated from point A and B result in an amplitude that is relatively depend on the positions of A and B and where new wave fronts are being observed. This is how the diffraction of x-ray solves the structure of molecules from single crystal.

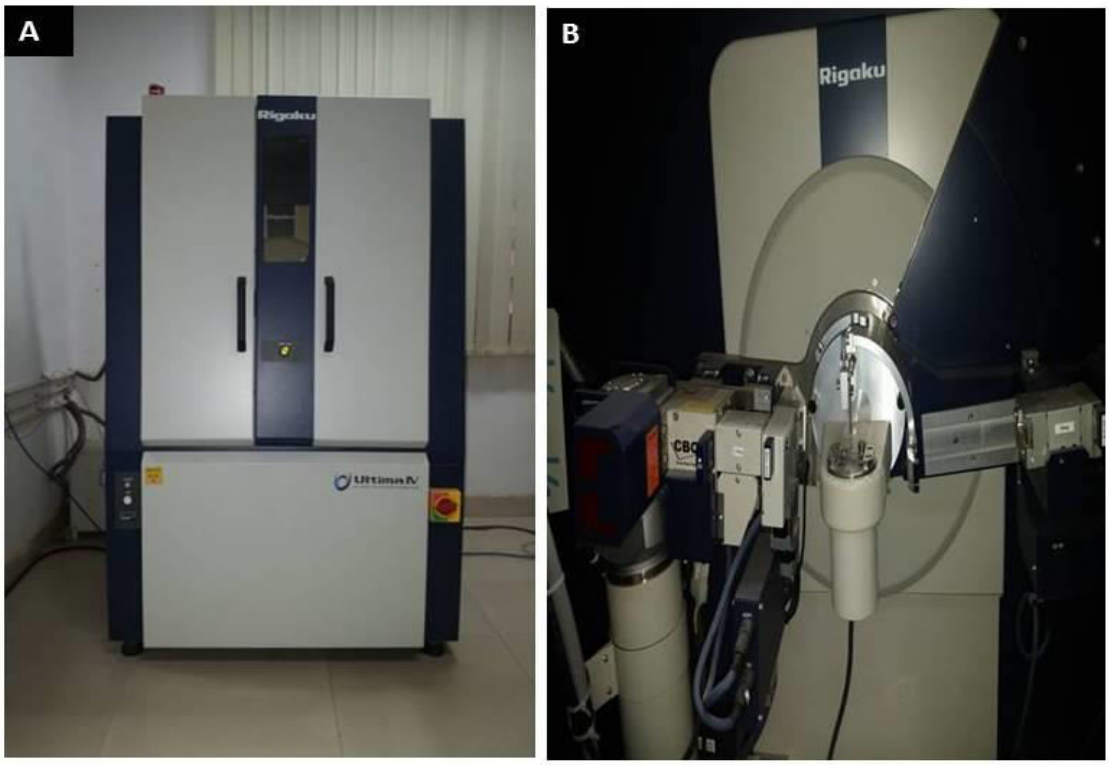

Figure2: Image of XRD instrument. **A**-The X-ray instrument, **B**- the X-ray beam generation chamber.

Bragg's law of x-ray diffraction:

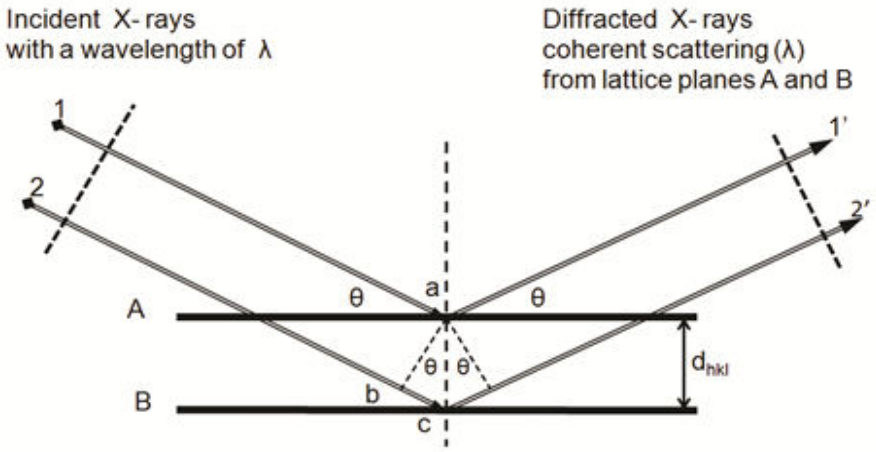

Figure3: Parallel lattice planes A and B showing the constructive interference of a front wave of parallel X-ray beam, 1and 2 are the incident radiations incidence at an angle of θ while 1' and 2' are the reflected radiations at an angle of θ.

W.L.Bragg developed a relationship to understand how diffraction relates to the relative positions of point objects in shape. To define Bragg's law of diffraction, lets assume lattice points on the crystal as parallel planes. Stacking a set of reflecting planes at regularly spaced intervals d creates a simple model of a one dimensional crystal. In this model a wave of x-rays with a wavelength λ is incident on the reflecting planes at an angle θ. The wave scattered from this plane is at an identical angle θ. But the question is which value of θ will result in constructive and destructive interference. As the distance between the parallel planes is d so the individual paths of the scattered light are parallel. Because we have a large no. of planes we observe constructive interference only when the reflected waves are perfectly in phase. This only occurs when the difference in the length of the path of the incident and reflected waves of each plane that is path difference (PD) is equal to some integer n of the wavelength of the incident x-rays.

$$PD = n\lambda$$

This path is related to the distance separating the reflecting planes by the relationship

$$\tfrac{1}{2}\, PD = d\sin\theta$$

$$= 2d \sin\theta = n\lambda$$

$$= 2\sin\theta = n\lambda/d$$

Larger spacing units in crystal result in smaller diffraction angle.

This principle of x-ray diffraction explains how diffractions through crystal determine the structure of molecules.

PRINCIPLE OF SEM

Figure4: The image of Scanning Electron Microscope

SEM stands for scanning electron microscope, is an instrument that scan the surface of the specimen,by a beam of electron, instead of light and that reflect to form an image. Now a days it is largely used in physical sciences and biological sciences for detecting the structures. SEM works by the coordinated action of seven primary operational systems. Vacuum, beam generation, beam manipulation, beam interaction, detection, signaling processing, and display record. The following components are present in a scanning electron microscope:

Figure5: Image showing electron flow chamber of SEM.

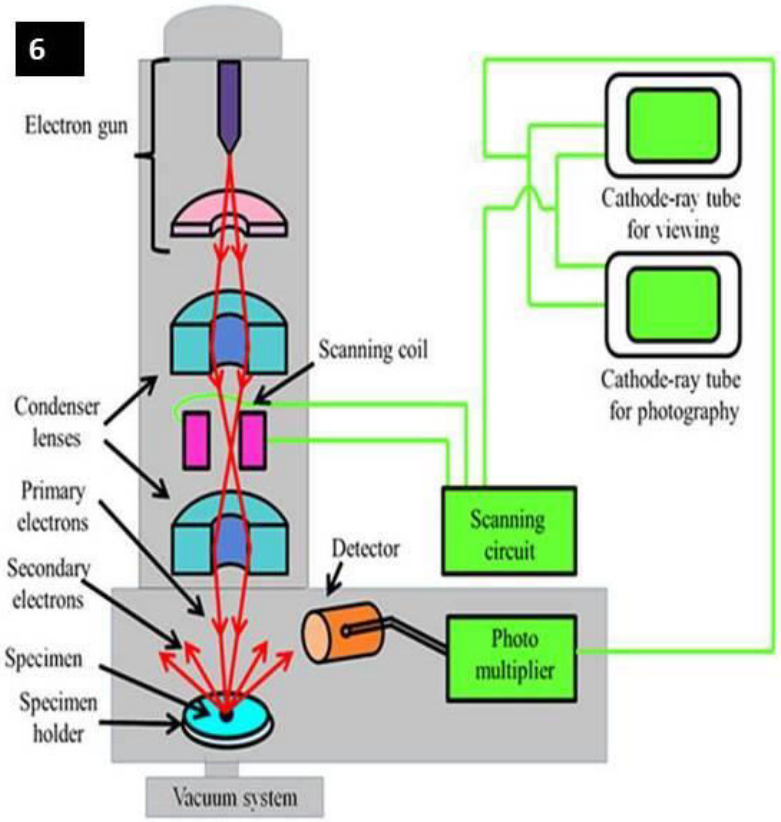

Figure 6: The schematic diagram showing function of SEM.

1.Electron column and beam generation:

Electron column is the region where electron beam generate under vacuum. The lower portion of the electron column contain specimen chamber. The secondary electron detector is located above the sample stage inside the specimen chamber. The electron gun is the beam generation system of an electron microscope. The electron gun consist of three components: a filament or cathode made of tungsten wire, Lanthanum Hexaboride (LaB6) crystal, or Cerium Hexaboride (CeB6), (2 C.E. Lyman, et al..1990) grid cap (Wehnelt Cylinder) that controls the flow of electrons and 3) a positive charged anode plate that attracts and accelerates the electrons down the column to the specimen. The electrons are generated from tungsten at 2700k. Tungsten is choosen as these filaments are little cheap to obtain and can be operated at less vacuum that is 10^{-4}torr of pressure. Disadvantage is that they have short life span. The electrons are emitted through thermal emission. The filament starts heating as current flows through it. As the current flow increases through the filament, the filament temperature increases. As the temperature increases the electron emission by the filament increases. But the electron emission occurs up to a certain point, beyond which the increase in filament current has no role on the electron emission; rather the filament may burn out. The point at which maximum emission of electron occurs with respect to increase in filament temperature is called saturation point. Increasing the temperature of filament above its saturation point will cause the decrease in life of filament. Adjusting filament current below its saturation point will cause the unstable beam current and poor image quality. Other two filaments have strong resolution, longer life span but they are extremely cheap. The filaments present inside the wehnelt cylinder which control, the number of electrons flowing from the gun. Primarily electrons are accelerated toward anode which is adjustable from 200v to 30kV.

There are two types of emission of electrons, one is thermal emission and another is field emission. We already discussed the thermal emission which is temperature dependent. Next is the field emission.

i)Field emission:

In this case heat is not used to excite the electrons from the filament. In field emission gun the electrons are said to be cold electron source as they don't require heat for emission as emission

in this case occur by strong magnetic field. The filament consists of a fine pointed tungsten wire (ideally one atom across at the tip), kept at a high negative charge along with the rest of the cathode. The anode is kept at a positive charge. The large difference in potential difference on a small point pulls the electrons out of the filament. The advantages to this system are that the emission is cool, the emitted beam is much smaller in diameter (better resolution), and filament life is generally longer. The disadvantages are a much higher vacuum (approximately 10^{-7}Torr) require and a cleaner microscope (special pumps not oil diffusion) is needed for operation. Any debris sticking on the fine tip of the filament will cause a reduction in emission. Debris will routinely stick to the filament. Thus the microscope needs to be cleaned out routinely to maintain a clean gun. Another disadvantage of field emission is long acquisition times during X-ray analysis. Field emission gun will not generate many X-rays since low beam currents and the small beam diameters are used.

ii) **Condenser lenses and electron beam manipulation**:

Two condenser lenses are there. After the beam passed through the anode it again travel through two condenser lenses in order to converge or narrow down the beams , so that it will pass through the focal point of lense. Along with the accelerating current, the lenses are used for determining the intensity of the electron beam when it strikes to the specimen (Postek, et al.1980).

iii) **Apertures:**

Depending upon the kinds of aperture can be used in the electron column. The aperture located below the scanning coil determines the diameter or spot size of the beam at the specimen. The spot size determines the resolution of the image. Lesser the diameter of the spot size more will be the resolution.

iv) **Scanning system:**

The image is formed when the electron beam scan the surface of specimen. There are two coils present in the objective lense for scanning and raster formation. One is rastering coil and other is deflecting coil. Deflecting coils are present to deflect the electron beam such a way in a multiple direction that it will focus on the scanning spot. The deflecting coils produce a uniform magnetic

field for the uniform movement of electron field. The rastering coil causes the beam to scan over a square area on the sample surface.

v) Specimen chamber:

Specimen chamber and its control are located at the lower part of the column. The secondary electrons from the specimen that is the electrons are obtained on specimen by coating are attracted to the detector by a positive charge.

2.Vacuum system:

High vacuum is needed to maintain the electron column in order to control the electron beam falling on the specimen. A high vacuum is maintained at a pressure of atleast of $5x10^{-5}$torr. High vacuum is required for the reasons like, first when the current passes through the filament cause the increase of temperature around 2700k.(2 C.E. Lyman, et al..1990). At this temperature and in the presence of air hot tungsten filament will burn out because of oxidation. The column optics need a clean and dust free environment in order to operate. The dust particle or air inside the column may block the path of electron beam before it reaches to specimen chamber (Postek, et al.,1980).

3.Electron beam and specimen interaction :

To get a good resolution an electron source is required instead of light source which can bring resolution up to 25A0. In SEM image can be visualized by two kinds of electron flow, secondary and back scattered electrons. These two kinds of electrons produced from the surface of specimen, but under electron beam they are result of two different interactions. Secondary electrons are a result of the inelastic collision and scattering of incident electrons with specimen electrons. They are generally characterized by possessing energies of less than 50 eV (Postek, et al.,1980). They are used to reveal the surface structure of a material with a resolution of ~10 nm or better (Postek et al.,1980). There are several types of signals are generated from the interaction of electron beam and specimen. One among them is X-ray, the only other signal which is used typically in SEM. The x-ray signal is the result of interactions between free electrons and positive electron holes that are generated within the material. The x-ray signal can originate from further down into the surface of the specimen surface and allows for

determination of elemental composition through EDS (energy dispersive x-ray spectroscopy) analysis of characteristic x-ray signals.

4.Accelerating Voltage:

The voltage can be adjusted between 200-30kV. Higher voltages (15- 30kv) generally give high resolution at high magnifications although; this can damage the specimen very quickly if it is not highly conductive.

5.Working distance:

Working distance and spot size will greatly influence the image quality. Generally a working distance of 10mm should be used and will allow for a good depth of field while maintaining good resolution. Working distance can be reduced in case of low accelerating voltage in order to get good resolution.

6.Spot size:

Spot size basically restricts the beam current and thereby cause for brightness and contrastness of image. Smaller spot sizes require higher brightness and contrast levels thus there can be a limits when using a small spot size. Typically smaller spot sizes allow for higher resolution and a greater depth of field.

MATERIALS AND METHODS:

Sample preparation for XRD:

For XRD analysis first the interested portions of the feather was cut, then put on the sample holder. The feather samples were scanned at an angle of 5 to 90 degree with a rate of 5 degree per minute and step size of 0.05 to obtain the XRD graphs. Then the graphs were plotted using Origin 8 software and elements were detected using EDX.

Figure 7: Sample holder of XRD

Sample preparation for SEM:

The feathers taken were dried and handled with gloves in order to avoid finger marks and dust. Samples were placed on sample holder using double sided conductive tapes. Vacuum compatible carbon black tapes were used. When samples are not very conductive, charge effect will cause image distortion or drift. Low acceleration voltage should be used to reduce the charge effect if samples cannot be coated with a conductive coating. To complete eliminate the charge effect, samples should be coated. SEM lab has coater for gold coating. The coating thickness could be several nanometer to tens nanometer depending on if the coating interfere with the morphology of your sample. After coating, the sample should be mounted with a conductive "bridge" (e.g. carbon / copper tapes, or silver paint) connected from the top surface of the sample to the sample holder. Then with sample holder placed inside the SEM and the images obtained on computer screen by operating with the software.

Figure8: Instrument for gold coating before SEM imaging.

Image j software:

Image J software was used to measure the lengths and angles of different structural components of feather like barb diameter, rachis diameter, barbule length , distance between two adjacent barbules and the angles that barbs making with rachis. For measuring various components following steps were performed , 1) the home page of ImageJ software was opened, ii) Clicked on file option and from the scrolled down menu, selected open, the image containing file was opened iii) analyze option of ImageJ home page was clicked. In the scroll down menu the set scale option was selected. The set was selected and same scale taken on the SEM images was and unit was given in µM and clicked on ok button. Scale was setted. Iv)The straight line was selected from the home page to measure the straight lines v) to measure the accuracy of the scale that was setted the length of the scale line appeared on SEM image was measured from beginning to end and then clicked on set scale to obtain its scale and then scale setted accordingly.vi)Then different components to measure were measured with the need of measuring parameters like angles or length in straight line and then clicked on analyze option from the home page of software and clicked on measure . The measured value was obtained.vi) For each

measurement 10 readings were taken and the average and standard deviation calculated to obtain the measurement of particular component.

OBSERVATION AND RESULT

Nape feather:

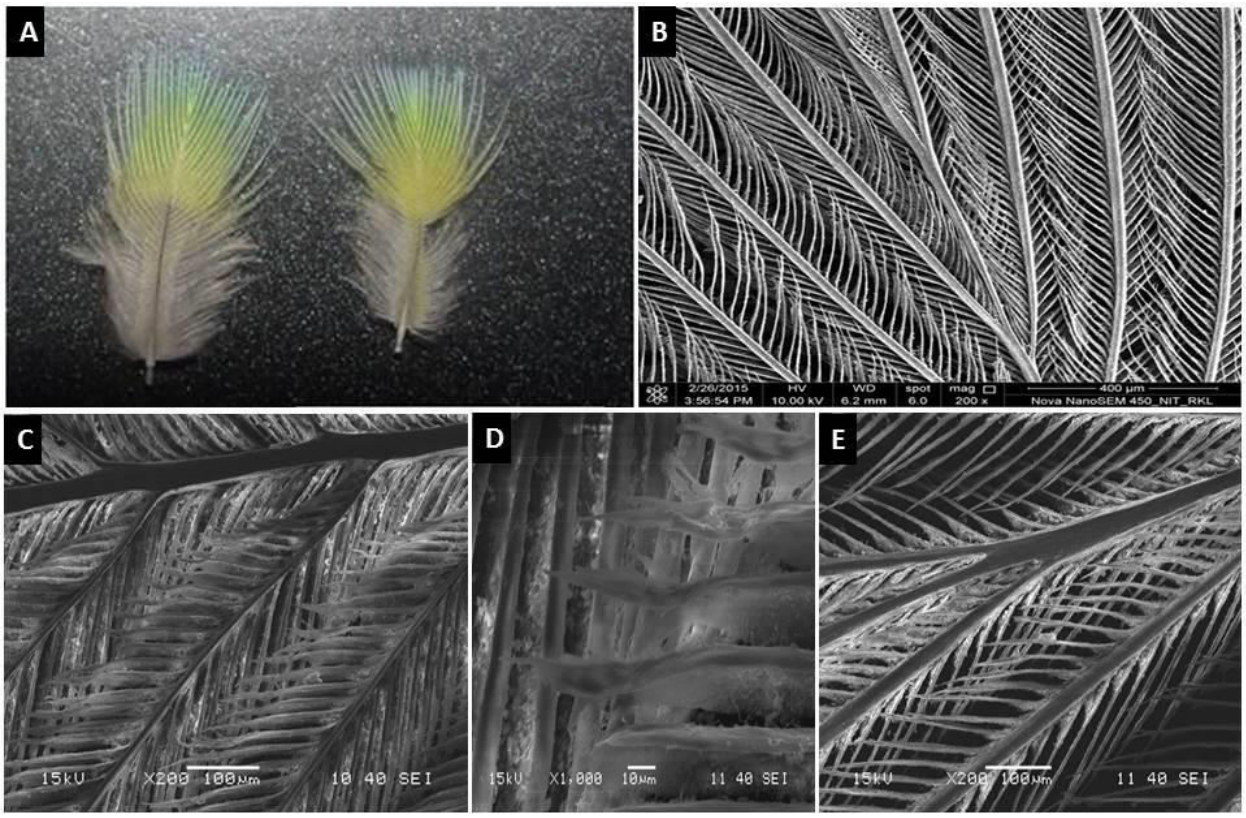

Figure 9: A-Feathers of nape region, B- Nape feather at 200x magnification and at a scale of 400µM showing the barbs and barbules arrangement at the transition greenish yellow portion, C- Arrangement of various structures of nape bottom (light yellow)feather shown at magnification of 200x at a scale of 100µM, D-The magnified structure of tip barbules of feathers collected from bottom of nape at a magnification of 1000x, E- The magnified image of tip portion of nape feather (sky blue) showing the arrangement of different components at a magnification of 200x and scale of 100 µM.

The nape feathers (**Figure 9(A)**) have a fan like structures with the feathers are spreaded outward at the tip portion shown in the figure1. The feathers are light sky blue in color at the tip portion

followed by a light yellowish green transition toward the bottom , the next portion present after this transition region toward the bottom is yellow in color , then the region present next to it toward extreme bottom is grayish white in color. In general half of the portion, these feathers toward the tip are colored while half of the portions toward bottom are grayish white in color.

The SEM images of these feathers were taken at an electron flow of 10.00KV. at a spot size of 6.0 with different magnifications at different scales too in order to study the arrangement of various components of feathers, which are done by nature at a nanoscale.

Unlike all feathers it **(Figure 9(B))** consists of a central shaft or rachis. The lower portion of the shaft or rachis is free from barbs or barbules and is called quillis. In the upper portion of feather the rachis gets thinner, tapered and branched toward the end. The rachis gives rise to barbs laterally and they are present parallel to each other by forming an angle with the rachis. Then barbs give rise to barbules, which are also arising laterally from the barbs. This gives the feather an appearance of branches of a coconut tree. The barbules of each barb are arranged in such a way that whole, together they look like veins of a leaf to naked eye. When this feather is visualized under SEM (200x) the nice structural arrangement of the barbs and barbules are visible Barbules of each barb generally form a pattern with its adjacent barbules present on both left and right side, by interlocking with each other. Each barb contains barbules on its both left and right side in a symmetric fashion. In each barb containing barbules, one row of barbule present on one side are exposed while other side is present beneath the adjacent barbules of just nearby barb. When we observed the arrangement of barbs and barbules on both side of the rachis an opposite pattern is viewed. On the left side of the rachis the barbules present on left of each barb are covered by its adjacent right barbules of the barb present just left to it. Hence the left barbules of one barb are interlocked beneath the right barbules of another barb just present left to it. But when we viewed on right side of the rachis we observed the just opposite pattern of arrangement of the barbules of each barb, that the left barbules are exposed while the barbules present on the right side of barb are present beneath the barbules of the barb just present right adjacent to it.

At the bottom of nape feather (**Figure 9 (C)**) a different arrangement pattern is observed, the structures of barbule components are also found to be different in these regions. The barbules which are exposed are flattened in shape from its base and elongated to a distance of 118.16±

10.09µM then tapered toward the end where the distance is calculated to be 66.36 ±11.63 µM .The diameter of rachis at this point is calculated to be 27.10 ± 3.82µM. Distance between two individual barbules is 13.80 ± 1.78µM. The diameter or thickness of the barbs present at nape bottom region is 6.72 ±1.18 µM. The angle that barbs at bottom nape region are making with the rachis is 42.42 ± 1.10µM. The distance between two barbs at nape bottom region of feather was calculated to be 304.08 ± 6.52 µM.

The structure and arrangement of barbules at higher magnification of 1000x and at a scale of 10µM was studied in (**Figure 9(D)).**In some of the barbules, at tip portion they became branched and in higher magnification it looks like an outgrowth from the branch. But this tip branching of barbules are not symmetric or regular. It varies from barbules to barbules. The flattened barbules are present obliquely and interlocked with each other. Very small air gaps are present in between two barbules viewed at 1000x magnification at a scale of 10µM.

The tip portion of nape feather which looks very light sky blue was studied at a magnification of 200x with a scale length of 100µM in the (**Figure 9 (E)).**The tip of nape feather contains a different type of barbules which are thin, long and similar as the middle nape feathers. The rachis at the top little thickened branched to give three barbs. The rachis along its entire length excluding the quillis portion lined with barbules. At the tip portion the barbules of barbs are interlocked with the immediate barbules that are arises from the rachis itself. At the sharp tip portion the barbules of each branched barb formed by the end branching of rachis are highly zipped with each other. The diameter of the tip portion of the rachis was measured to be 29.78 ± 7.36 µM. The diameter or thickness of the barbs at the tip portion of nape feather was found to be 19.86 ±3.50 µM. The diameter of rachis at the tip branching portion is found to be 30.61 ± 1.13µM. The distance between two barbules at nape tip feathers is found to be 14.99 ±2.36µM. At the extreme end point of rachis at the nape tip region, the rachis is branched to give two barbs. These two barbs are arise from a same point of rachis. The diameter of these two barbs were calculated to be 14.78 ±3.78µM

Red collar feather:

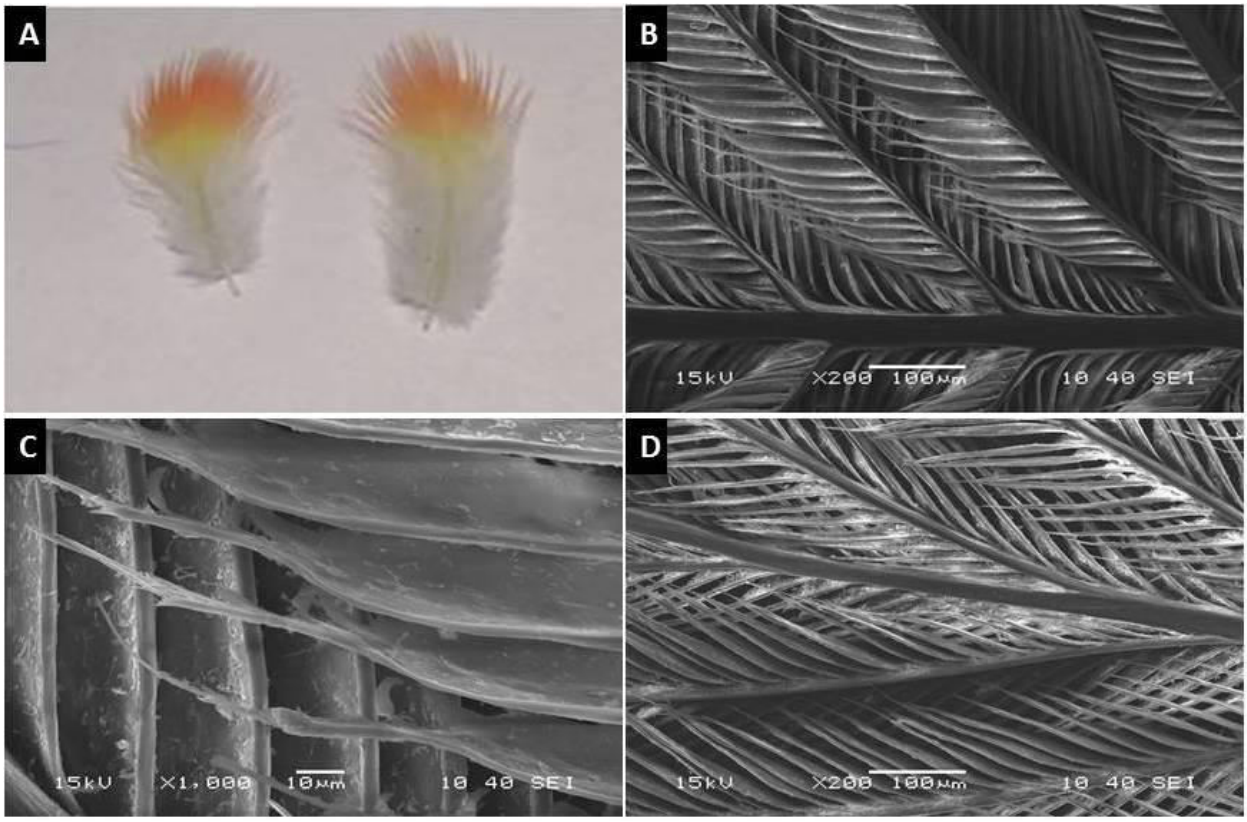

Figure 10:A-The red feathers of the collar ring region, B-yellowish green part of Red collar feather bottom magnification of 200x and scale distance 100µM, C- The tip portion of the barbule of collar (yellowish green) bottom magnified. Image taken at 1000x magnification at a scale of 10µM, D-Collar tip reddish orange region at 200x magnification and at a scale of 100µM.

The collar feathers (**Figure 10(A)**) are reddish orange in color at their tip and their arrangement give the red ring like structure in parrot's neck only in male. Individually the feathers of this region show three types of coloration. The tip portion is red, followed by a greenish yellow transition next to it toward the bottom then finally followed by white color toward the end or extreme bottom. These are small and thin feathers. The rachis in the middle looks light yellowish green in color.

The feathers at collar region are red. The SEM image of the red feathers at collar region is taken at 200x magnification and at a scale of 100µM with a spot size of 6.0.

The diameter of the rachis at collar bottom (**Figure 10(B)**) was calculated to be 35.21± 2.49µM. From the rachis barbs are arise from both sides alternate to each other. The diameter of barbs were measured and calculated to be 9.21±2.70 µM. The barbules are flattened in shape from the beginning that is from the base, then at the terminal end these are narrowed to form a thread like thin structure. Hence it can be said the barbules have two parts one is anterior wide and flattened part and second posterior terminal thread like part. These thread like structures in some barbules are extended to reach the adjacent barb present near to it. The length up to which the flattened portions of barbules are extended measured and calculated to be 128.94±9.51µM. The length of the tapered thread like part of the barbule were measured and calculated to be 79.28±12.48µM. The exposed body surface width of the exposed barbules were measured and calculated to be 16.58±3.06µM. The distance between two adjacent barbs in these feathers was measured and calculated to be 216.74±6.30µM. In this feather the barbules form a uniform arrangement by overlapping on the barbules of adjacent barb. The barbules which are exposed visible entirely with all its structures and the barbules which are present underneath expose the base portion only , while the remaining portions are covered by the nearby barbules.

The thread like tip portion of the barbules are magnified to 1000x at a scale of 10µM (**Figure 10 (C)).** It was observed that the point from where the thread like elongated tapered structures arises from the flattened barbules , are associated with another outgrowth like structure along one side which can be visualized as a bifurcation. The elongated thread like tapered end and barbules are highly irregular and gives rise to many outgrowths like structures along its entire length and pointed toward end. It can be observed from the above image the flattened end of barbules is bifurcated at one end to give the elongated thread like structure while the other side is placed at its position as such, and tapered to become pointed.

At the tip portion of collar feather the rachis is more branched (**Figure 10 (D)).** The diameter of the rachis was measured and calculated to be 30.96±3.05µM. At the tip of the collar the rachis is highly branched to give many barbs which form a canopy like structure at the top. Toward the tip of the collar feather the rachis becomes thinner and the diameter can be measured and calculated as 20.57±2.34µM. The diameter of the barbs measured and calculated to be 11.04±1.76 µM. The

barbules present at this region are observed to have a different structure, than the one present at bottom. These are thinner and less flattened than the structures found at collar bottom region. As observed from the image, barbules of this region become thinner from base to the tip gradually in a uniform way and pointed at the end. In this image it can be observed that there present some spaces between each adjacent barbules at top although they are not uniform. The distance between the barbules at tip measured and calculated to be 16.38±3.85 µM. At the tip the barbules were observed to show a highly interlocked structure, with the barbules at one side of barbs are exposed and the other side was falling beneath the barbules of adjacent barb.

SEM ANALYSIS OF SHOULDER FEATHER:

The feathers from the shoulder region were collected (**Figure 11 (A)).** These are the tiny and thinnest feather of the parrots. They look grayish green in color. The tip portion is light faded green. Then it is followed by a light grey coloration toward the base. The feathers are wide, curved with a blade like structure. Even though all these feathers are collected from the same part of body, still their pattern of coloration and their shape varies from each other which can be visualized from the original feather images of figure 11(A). All these feathers are curved from their lateral dorsal side. Some feathers are curved bulged out laterally from right edge and some are from left edge and some are uniform along its both edges.

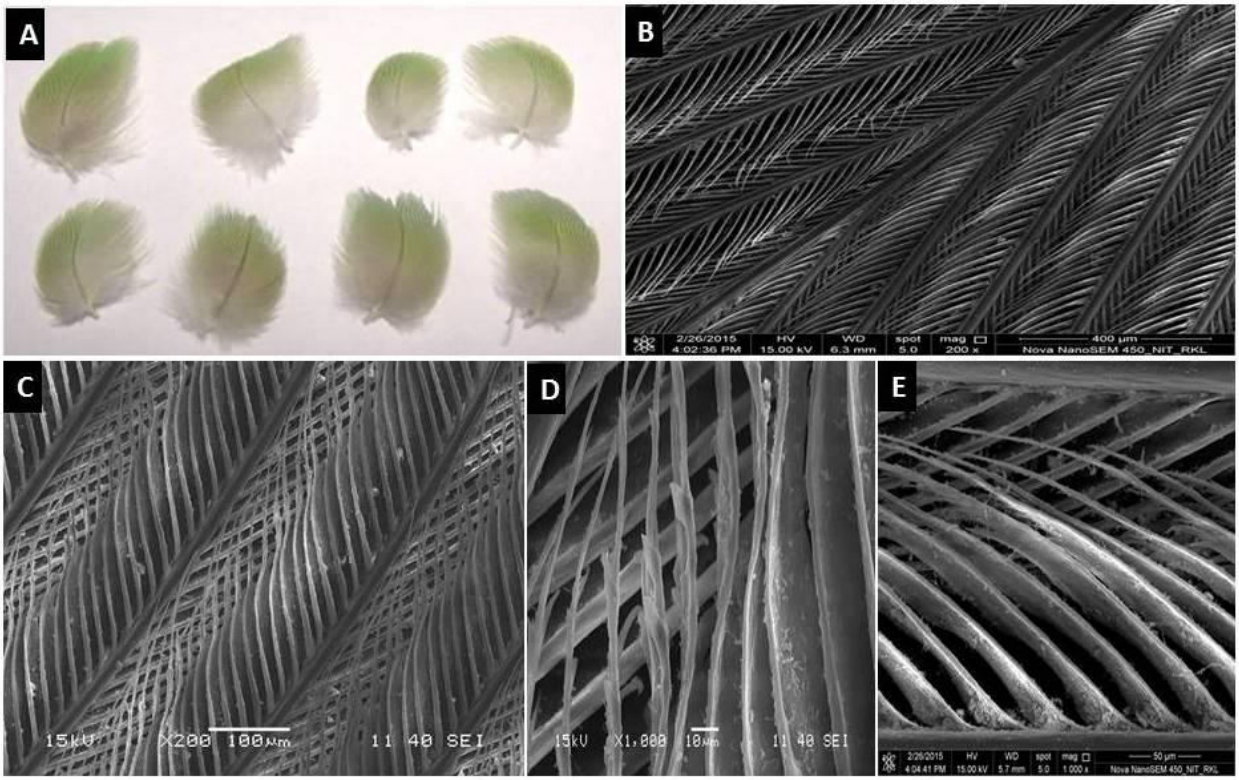

Figure 11:A- Feathers of shoulder region, B-Image of tip portion of shoulder feather at 200x magnification and at a scale length of 400µM, C- The SEM image of shoulder feather green region taken at 200x magnification at a scale of 100µM at electron flow of 15kv, D-Magnified image of barbule tip part at 1000x magnification and scale length of 10µM, E-Magnified image of tip barbules of shoulder feather magnified at 1000x at a scale length of 50µM.

To understand the nanostructure arrangements of various components of these feathers their SEM analysis was done. The images were taken using Scanning electron microscopy at various magnifications and scales at the spot size of 6.0.

In the above image (Figure 11 (B)) it can be observed that in tip shoulder feather at tip portion the rachis is highly branched to form barbs. This may be responsible for width of the feathers at the tip. The angle at which barbs arise from rachis at the tip measured to be 13.18±2.25 µM.

The feather was viewed at 200x magnification at a scale of 100µM (**Figure 11 (C)).** In this figure the barbs and barbules shape arrangement were focused. The diameter of the barbs were measured and calculated to be 16.72±1.81 µM. The barbules are flattened curved plate like structures. The distance between two barbules aligned side by side measured and calculated to be

16.00±1.73 µM. Barbules are flattened and curved from its outer side toward the end. The flattened shape of the barbules extended up to a certain length then becomes tapered gradually to give long thread like structures. It was observed that there thread like structures arise from the terminal end of flattened portion of each barbule by forming a tube like structure. It was observed that the flattened barbules at their terminal end bifurcated to give the tube like base structure of elongated thread like pat of barbules. The other part of the bifurcation looks like a small outgrowth and present at its original portion as usual and pointed at the tip. The arrangement of barbules seems as if adjacent barbules laterally overlap with each other side by side. The flattened part of barbules extended up to a certain length of 175.58±7.83 µM. The length of thread like part of barbules from its tube like base was measured and calculated as 153.14±17.07µM. The exposed barbules fall over the adjacent barb containing barbules, and the thread like part of the barbules elongated to the barbs fully covering the base of the nearby barbules of adjacent barb. In this case the barbules which are present beneath are completely covered by the adjacent barbules that are exposed. The overlapping of barbules of adjacent barbs in these feathers is shown to form a regular and beautiful interlocking pattern. The thread like part of barbules of one barb when overlap on flattened base of the barbules of adjacent barb, it form a regular arrangement pattern forming regular rectangular structures and a good interlocking pattern.

Thread like parts of barbules were magnified at 1000x at a scale of 10µM (**Figure 11 (D)).** The image obtained shown the fine structure of thread like part of barbules. Many outgrowths were shown to arise from the thread like part of barbules and are irregular on its entire length .These falls over, the obliquely arranged barbules, of its adjacent barbs to form rectangular structures.

The barbules present at the terminal end portion of the shoulder feather shows a different structure when viewed at 1000x magnification at a scale distance of 50µM (**Figure 11(E)).** Barbules show four different major shapes along its entire length. They are observed to be wide at base, then little thinner above to it, again wide and flattened above to it then gradually tapered to become pointed toward the terminal end. The surface thickness of tip barbules at its sharp base near the barb measured and calculated to be 28.85±2.23µM .The surface width of wide portion of barbules just above the sharp base was measured and calculated to be 15.03±0.85µM. The surface width of the little thinner portion present next to the second wide base region was

measured and calculated to be 10.07±1.99µM. The surface width of wide portion of barbule just present above the thinner portion was measured and calculated to be 16.29±1µM. The surface width of the region fourth measured wide segment of barbule was measured and calculated to be 11.12±1.77µM. The surface width of the tube like base of thread like part of barbule was measured and calculated to be 4.60±1.44µM. The body width of thread like part of the barbules measured and calculated to be 2.76±0.31 µM. In the image the open space between two barbules clearly can be observed at the base. The distance between two barbules or the open space present between them measured and calculated to be 10.97±1.68µM.

WING FEATHERS:

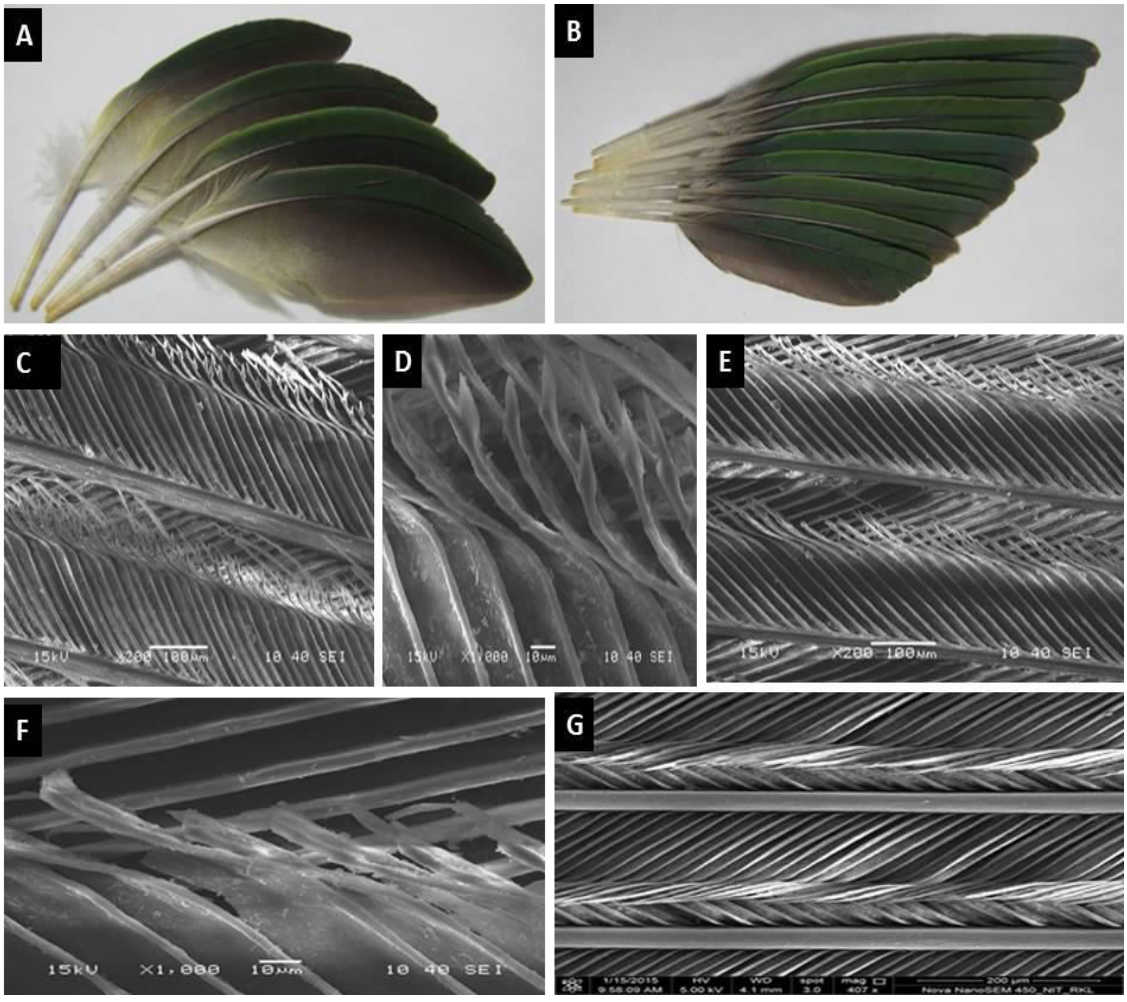

Figure 12- Different parts of wing flight feather. A, B- Flight feathers, C- The SEM image of the black portion of flight feather was taken, D- SEM image of tip of barbules of wing black portion

at 1000x magnification and at a scale length of 10µM, E- SEM imaging of wing yellow portion at 200x magnification and a scale length of 100µM, F- SEM image of tip portion of barbules of wing yellow feathers were taken at 1000x magnification at a scale of 10µM, G- SEM image of wing green region of flight feathers at a spot size of 3.0 at 400x magnification and at a scale length of 200µM.

Wing feathers (**Figure12(A), (B)**)are the strongest feathers and play a major role in bird's flight. These feathers exhibit three kinds of coloration, green, yellow and black. They show a vein asymmetry due to the unsymmetrical placing of the rachis. The rachis is placed asymmetrically to give a small vein upper one exhibiting green color and a larger vein lower portion showing yellow and black colorations. The quillis is thick downward showing its strangeness. It resembles like leaf in its shape.

The SEM imaging of different portions of this feather that is the yellow, black and green were done to understand the structure and pattern of arrangement of various components.

Wing black:

The black portion of the flight feather was imaged to unravel the arrangement of these feather components. The SEM image was taken at 200x magnification at a scale of 100µM and at an electron flow of 15KV (**Figure 12 (C)).** The barbules of this region are different from the barbules of different feathers. The average diameter of the rachis was measured and calculated to be 32.86±2.00µM. The barbules are long parallel scale like structures with thin thread like terminal ends. The terminal thread like ends of barbules are long and highly branched giving appearance of flower or leaf buds. The distance between two adjacent barbules measured and calculated as 12.39±2.50µM. In this case the flattened portions of barbules are parallel and uniform throughout without any laterally curved surface. The length of the flattened plate like portion of barbules were measured and calculated to be 183.01±3.77µM. As shown in the above image (Figure 12(C)) the terminal thread like end of barbules show unique variation in their length as well as structure. Some of the barbule terminals are longer and some are smaller, hence shows a variation. The average length of smaller length thread like end of barbules were measured and calculated to be 91.15±10µM. The average length of longer barbules were measured and calculated to be 156.15±71.30µM. A huge variation in length was observed. The

barbules were imaged at 1000x magnification and a scale length of 10µM (**Figure 12 (D)).**The image shows heading toward the tip portion the barbules are folded. The tip portions of barbules are highly branched and resemble some flower bud or leaf bud like structure.

Wing Yellow:

The SEM imaging of the wing yellow portion was done to understand the arrangement of various structural components of this part of feather (**Figure 12 (E)).**The diameter of barbs of this feather were measured and calculated to be 17.71±1.70µM approximately. The structure of barbules of this region also shows a different shape than the wing black region. The distance between two barbules measured and calculated to be 14.26±1.90µM. The barbules are parallel and scale like in shape. The length of flattened portion of barbules measured and calculated to be 207.95±6.76µM. The length of terminal part of the barbules measured and calculated to be 85.66±24.12µM. The terminal barbules of this region show high variation in their length.

The above image (**Figure 12 (F)**) shows the arrangement of barbules at its tip portion. Toward the tip the barbules are folded, remain thick and are not pointed like other feathers. The barbules in this figure are unbranched.

Wing green:

The SEM imaging of the green region of the wing feathers were done to unravel their structural components and arrangement (**Figure 12 (G))** at a spot size of 3.0 at 400 x magnifications and at a scale length of 200µM. This region shows a very different and unique shape of various structural components and their pattern formation. The barbs are parallel to each other and the diameter was measured and calculated to be 36.72±2.02µM. The barbules are long structures with two parts, the proximal flattened parallel plate structures and the distal thin part curved with certain angle, overlap on the adjacent barbules. The tip parts of barbules are remaining in an elevated condition instead of overlapping. The length of flattened parallel part of barbule measured and calculated to be 186.93±3.53µM. The length of terminal thin portion of barbules were measured and calculated to be 118.81±24.64µM. The ends of barbules seem to be overlap on the barbules of adjacent barb in a symmetrical fashion. The length of exposed base portions of

underneath barbules were measured and calculated to be 70.37±6.17µM. The distance between two barbules from their bases were measured and calculated to be 15.39±2.40µM.

TAIL FEATHER:

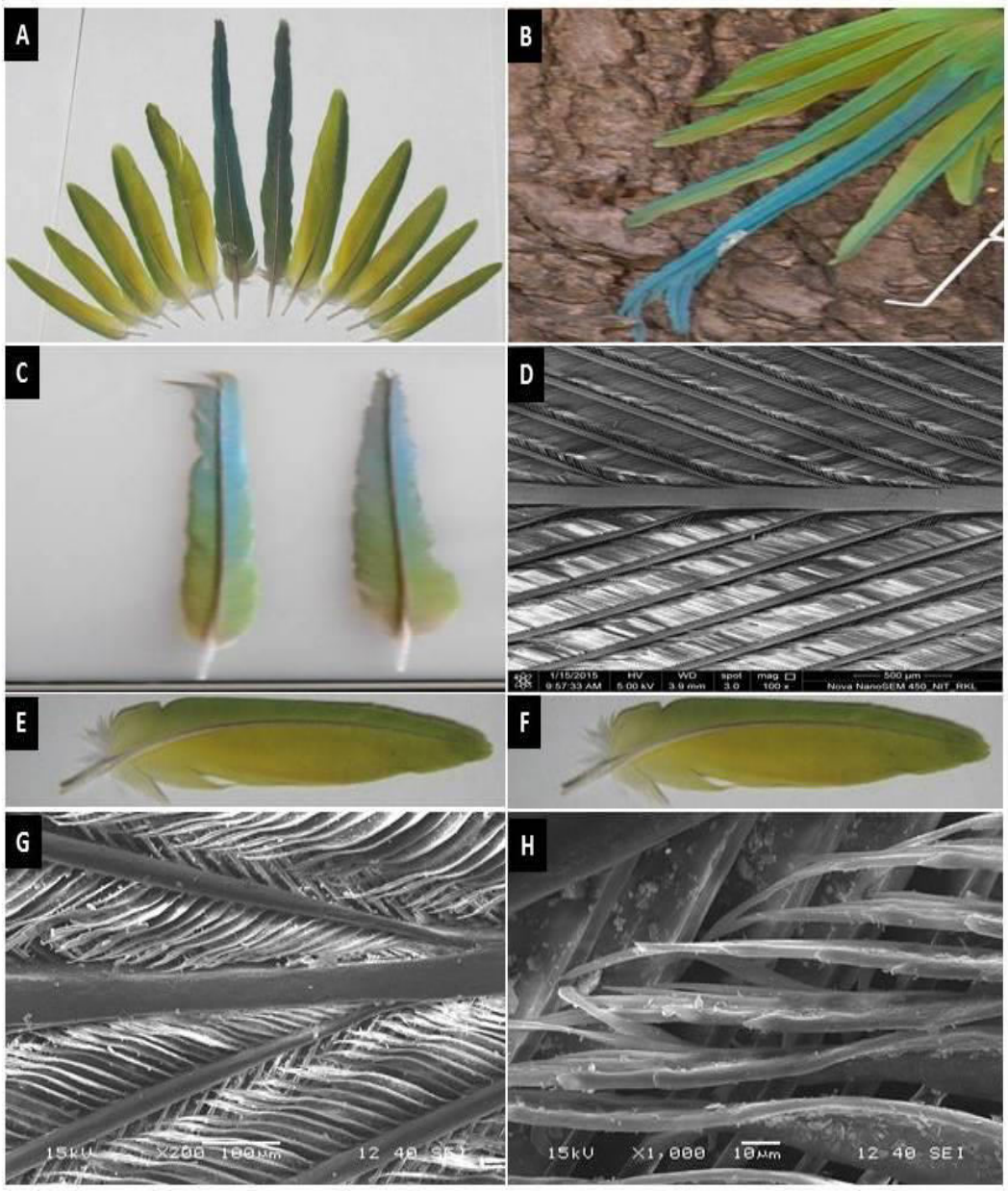

Figure13: A- Tail feathers image taken after arranging the feathers, B- Tail feathers, image taken directly from the parrot, C- Long sky blue graduated tail, D- SEM imaging of long sky blue tail at 100x magnification, scale length of 500µM at a spot of 3.0. , E,F- Side back green tail feather. G- The side back green tail feather at a magnification of 200x and a scale length of 100µM, H-

The structure of barbules of side back tail green feather at a magnification of 1000x at a scale of 10µM.

Tail is made up of 10 feathers two long sky blue feathers and 8 side light green feathers (Figure 13 (A)). The long sky blue tail feathers are the longest feathers present in pair one above the other at tail region. These feathers are present at the middle and surrounded by 10 side feathers from both sides, 5 feathers from left and 5 feathers from right. All the feathers present both at right and left are arranged in an ascending way in a gradually increasing size toward the middle large sky blue feather. The long sky blue feather is bifurcated at the end. It has a long rachis. In the above images it can be seen all the feathers show a different color pattern when they are viewed through different angles. The side back feathers which appear green in the (**figure 13 (A)**)exhibit a different coloration pattern of yellowish green vein at one side and yellowish green and sky blue combination at other vein along the rachis in (**figure 13(B)).** The SEM analysis of this long sky blue feather was done to understand the arrangement of the various structural components of this feather.

Long Sky Blue feather:

The SEM imaging of the long sky blue feather (**Figure 13(C)**) was done to unravel its structural components and their arrangement. The SEM imaging of the long sky blue tail observed to consist of a middle long rachis (**Figure 13(D)).** The diameter of rachis was measured and calculated to be 136.52±14.60µM. Barbs arise laterally from the barbules and are parallel to each other. The diameter of the barbs were measured and calculated to be 38.65±3.09µM. The barbs at their bases from origin are thin and thicken gradually on elongation. The distance between two barbs from base were measured and calculated to be 594.36±36.05µM. The distance between two barbs when they are parallel to each other was measured and calculated to be 198.11±7.57µM. The average angle that the barb is making with the barbules were measured and calculated to be 20.50±0.68 degree.

Tail side back green feathers:

The SEM imaging of the side back tail feather surrounding the long sky blue tail was done. There are eight side back green tail feathers surrounding the long sky blue graduated feather

from its both sides (**Figure 13 (E,F)).** The image was taken at an electron flow of 15kV at a magnification of 200x and a scale length of 100µM (**Figure 13 (G)).** The structure and arrangement of various tail components of this feather were viewed. It has a middle rachis which is thick at the region where it gives rise to the barbs. The rachis of this feather shows a unique feature that in between two barbs, it becomes thinner in its diameter toward the middle. The diameter of the end thicker portion of rachis were measured and calculated to be 60.56±4.18µM when viewed at 200x magnification. The diameter of the thin middle portion of rachis were measured and calculated to be 48.15±2.28µM. The barbs are arise alternatively from the rachis along each side and the arrangement is such that one lie just above the other one along the alternate sides. The barbs are thin at base that is at the point of origin and gradually becomes thick toward the tip as they elongate and after elongating a certain length they become constant toward the tip. The diameter of the barbs at the base were measured and calculated to be 13.84±2.11µM. The diameter of the middle transition portion of barb that is the region between thicker posterior portion and anterior thinner base were measured and calculated to be 26.00±1.00µM. The diameter of the posterior thicker portion of barb were measured and calculated to be 32.38±2.44µM. The distance between two barbules were measured and calculated to be 15.14±2.24µM. The barbules are flattened, elongated to a length of 143.55±5.92µM and further elongate to a length of 72.05±7.72µM and fold toward the end instead of giving thread like structure.

When the structure of tip portion of barbules of side back feathers were imaged at 1000x magnification at a scale length of 15kV unique structures were observed (**Figure 13 (H)**)The tip portion of the barbules of side back green feathers are folded structures and at the tip the barbules become branched to give finger like structures. Each barbule divides to give 6 finger like projections at the tip. The structure of barbules at this region shows a unique pattern than rest of feathers.

XRD Result analysis:

XRD analysis of feathers was performed on various parts of parrot's body feathers. At various wavelength peaks were obtained when the light passed at an angle of 2θ. The peaks were analyzed by using EDX software and a list of various elements were obtained. The functions of these elements in birds were proposed based on their antimicrobial properties or for coloration of feathers.

XRD graph of feather's from different region:

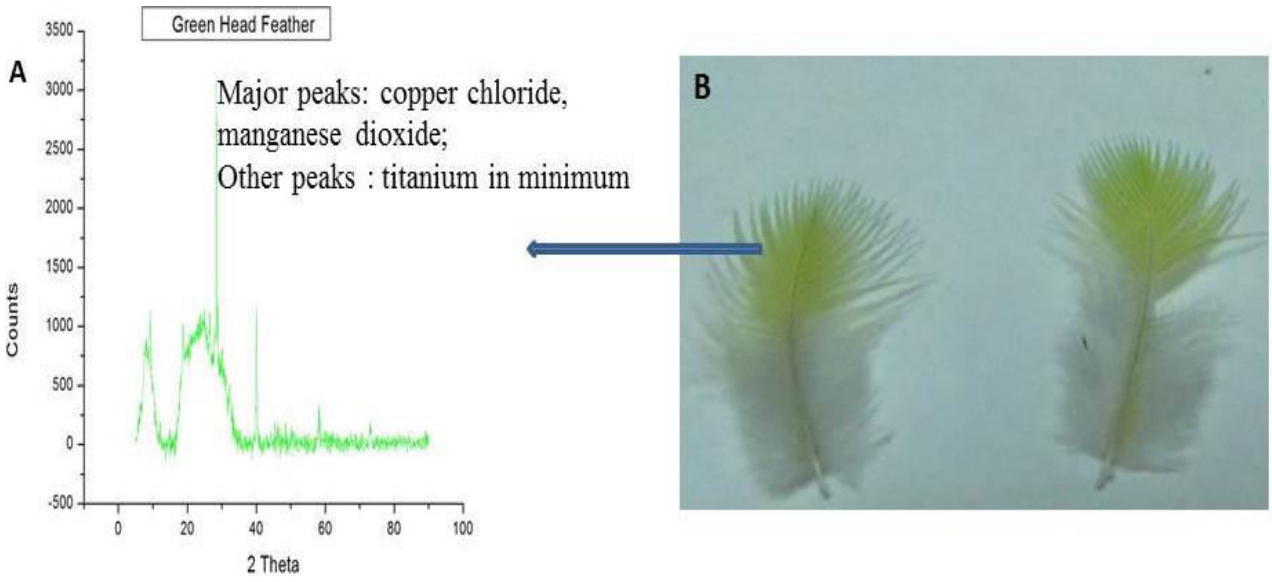

Figure 14:A-The XRD image of upper green portions of head feather and elements present in it. **B**- The image of head feather of *Psittacula krameri* visualised in naked eye.

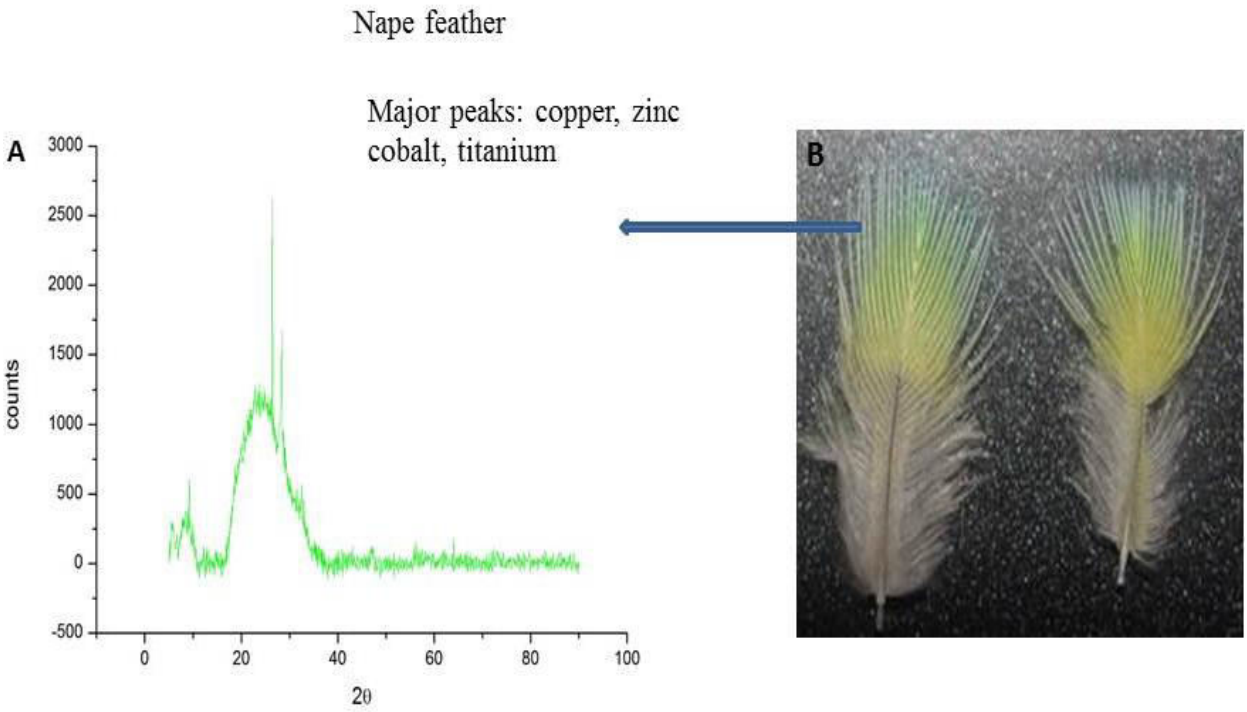

Figure 15: A- The XRD image of upper colored portion of nape feather and elements present in it, **B-** The nape feather of *Psittacula krameri* visualised in naked eye.

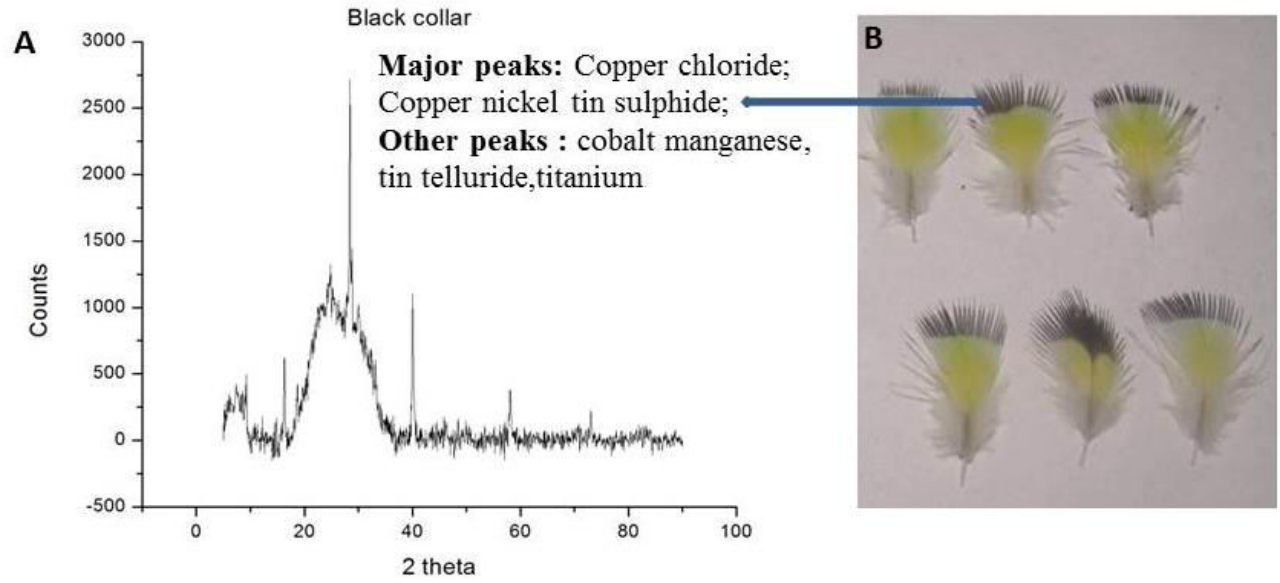

Figure 16: **A-** The XRD image of upper black portions of collar feather and elements present in it, **B-** The black collar feathers of rose-ringed male parakeet (*Psittacula krameri*) visualised in naked eye.

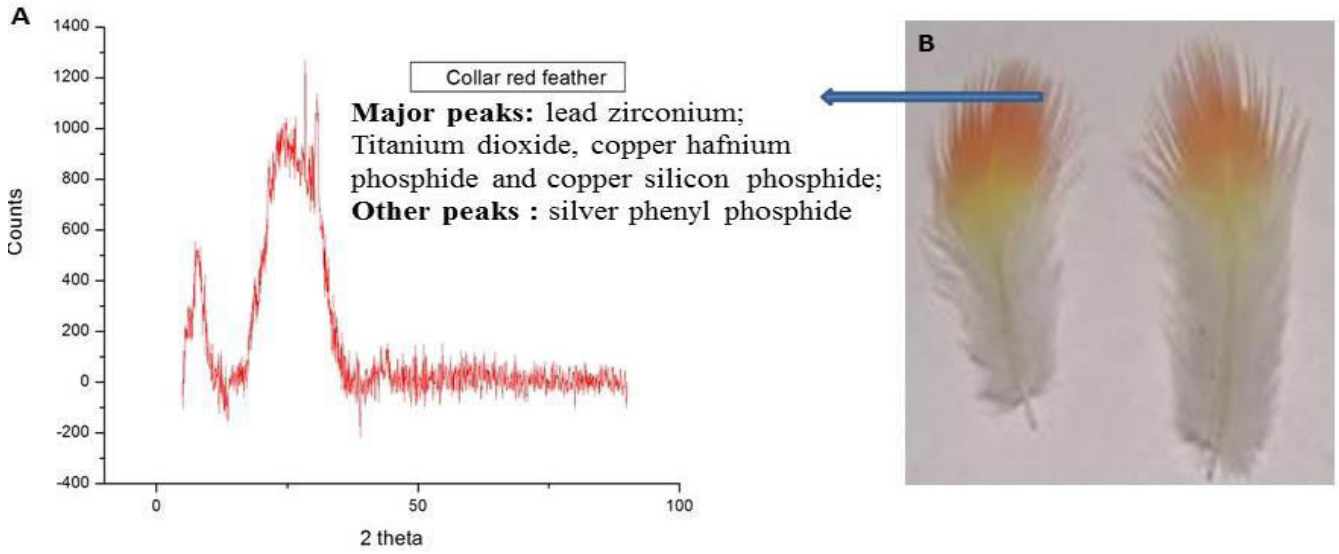

Figure 17: A-The XRD image of the tip red portion of red collar feather of male rose-ringed parakeet (*Psittacula krameri*), **B**- The collar feather of male rose-ringed parakeet (*Psittacula krameri*) visualized in naked eye.

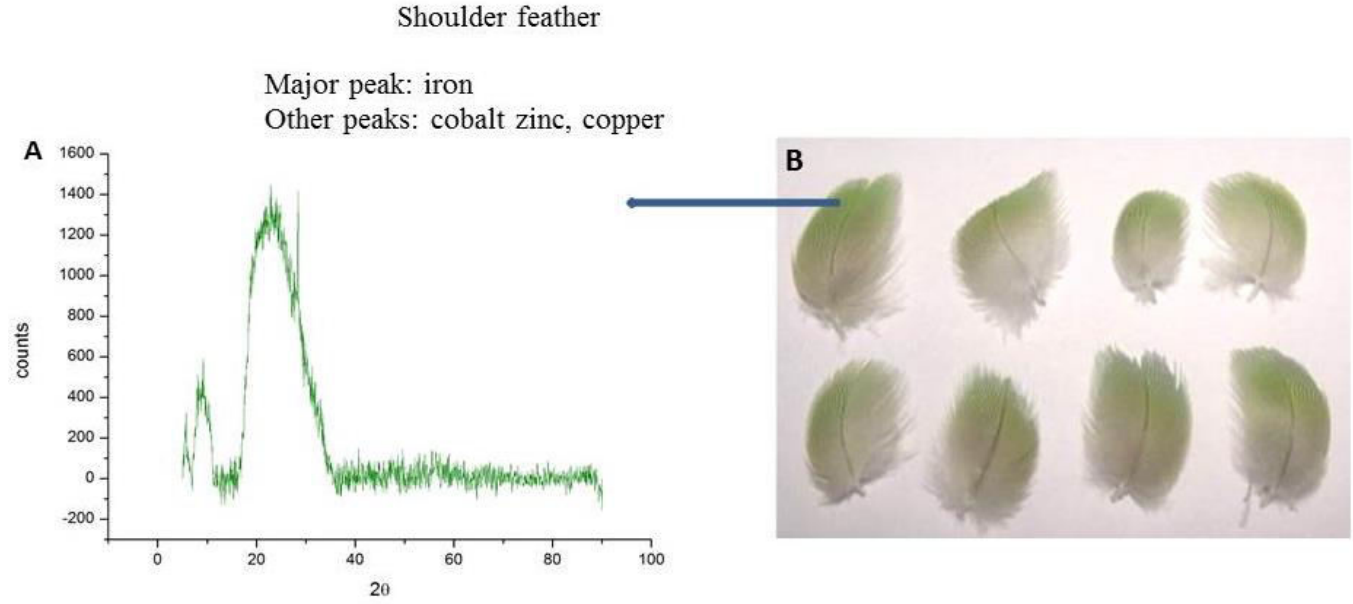

Figure 18:A-The XRD image of the tip green portion of shoulder feathers of *Psittacula krameri* and elements present in it, **B**- The shoulder feather of *Psittacula krameri* visualised in naked eye.

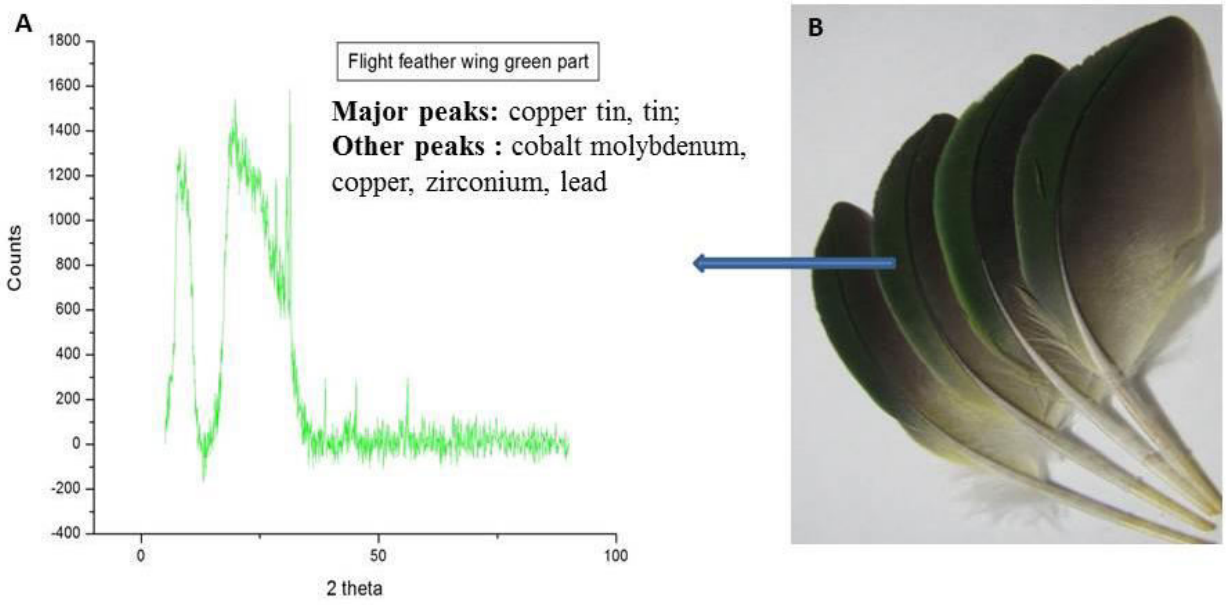

Figure 19:**A**- The XRD image of green portion of flight feather, **B**- Wing flight feather of *Psittacula krameri* visualized in naked eye.

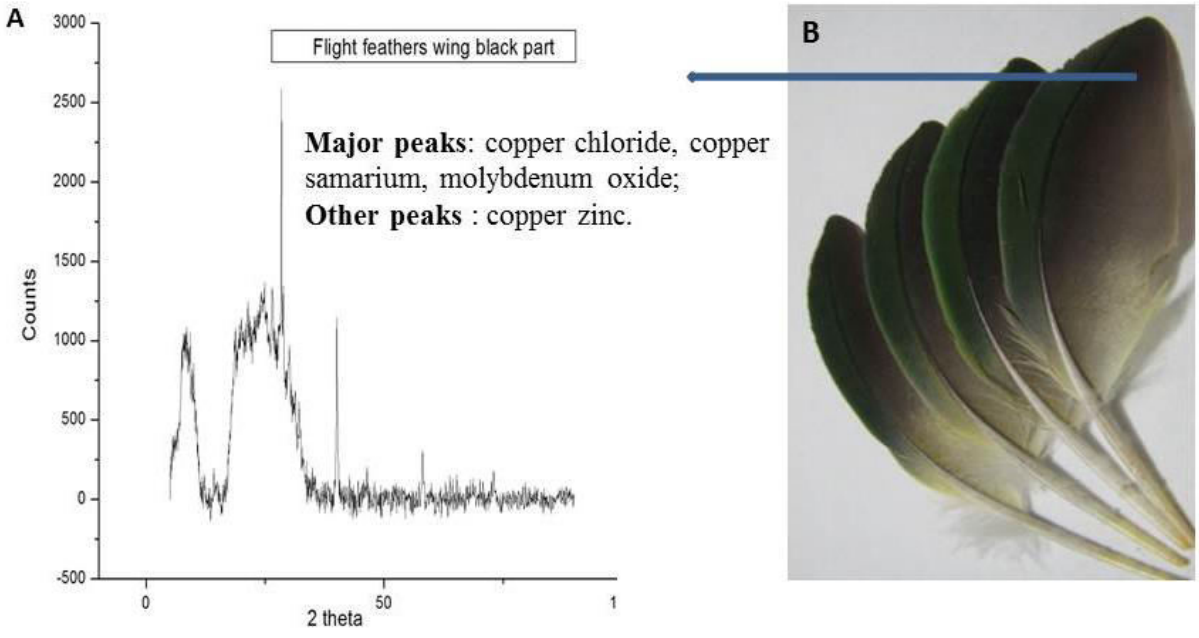

Figure20: **A**-The XRD image of black portion of wing flight feather and the elements present in it, **B**- The wing flight feathers of *Psittacula krameri* and arrow mark shows the black portion.

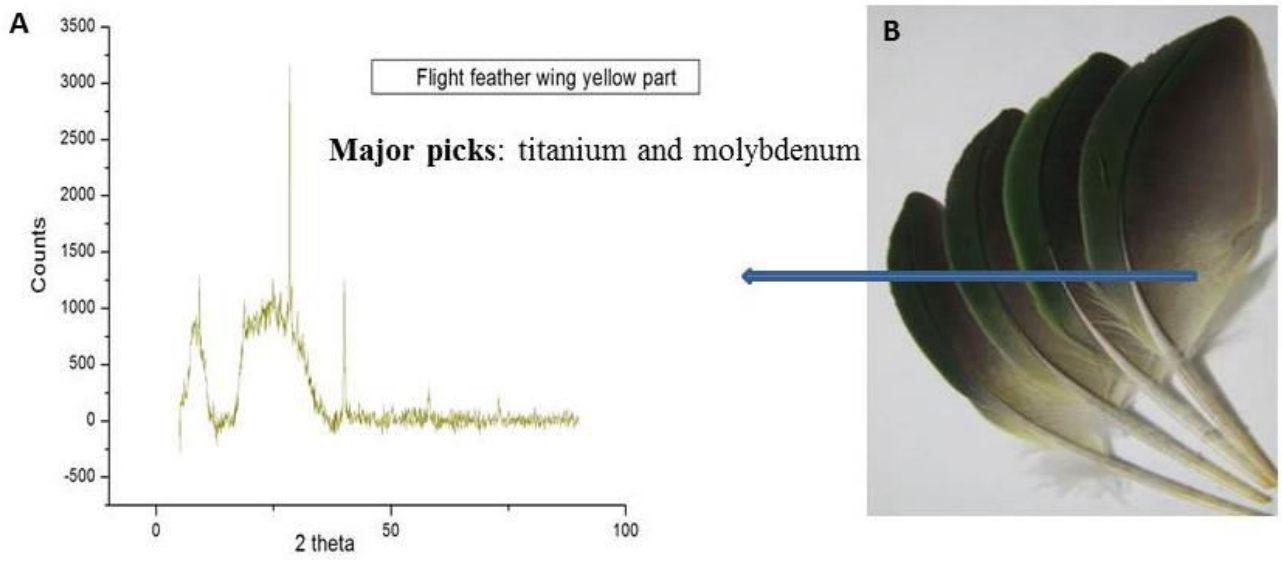

Figure 21:**A**- The XRD image of yellow portion of wing flight feather, **B**-The wing flight feather of *Psittacula krameri* visualized in naked eye.

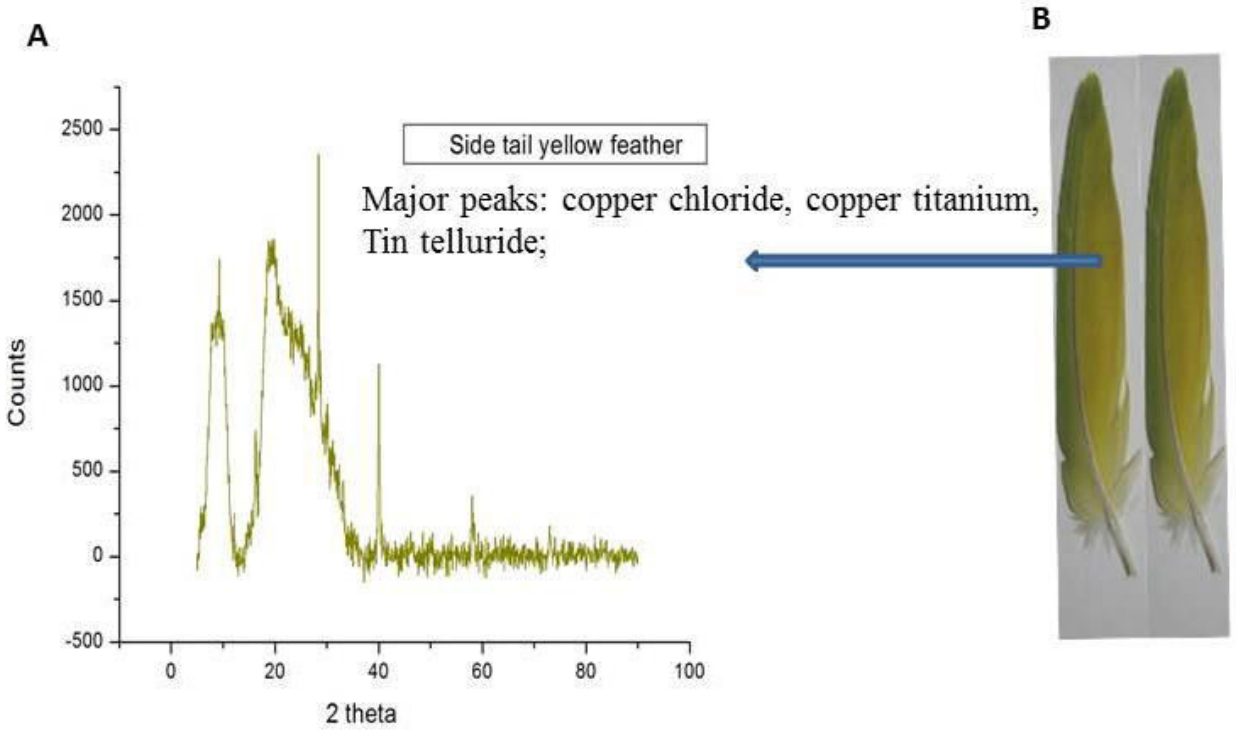

Figure 22: **A**-The XRD image of back side tail greenish yellow feather and the elements present in it, **B**- The back side tail yellow feather of *Psittacula krameri* visualized in naked eye.

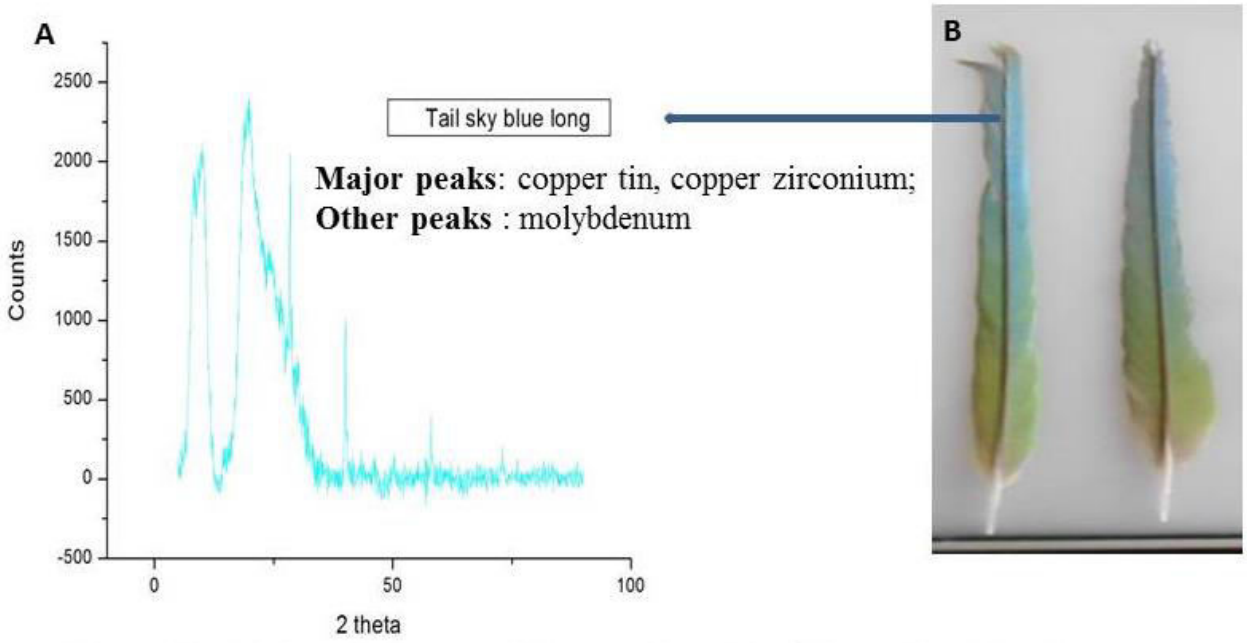

Figure 23: **A-** The XRD image of long graduated sky blue tail and the elements present in it, **B-** The long graduated sky blue tail of *Psittacula krameri*.

From the XRD graph the major elements listed from various feather peaks are mainly Copper, chloride, Titanium, Tin, Tellurium, Zirconium, Cobalt, Silver, Nickel , Manganese, lead, Molybdenum, Zinc and Iron. They are expected to have antimicrobial function and some of are listed below.

Copper chloride:

In early 19th and 20th century copper and its various inorganic derivative complexes were widely used in medicines in order to treat against diseases like eczema, chronic adenitis, scrofulosis, impetigo, tubercular infections, anemia, lupus, facial neuralgia and syphilischorea, (Dollwet and Sorenson 1985).In this way copper was used as an antimicrobial agent and this trend was continued up to the invention of antibiotics (Grass, Rensing et al. 2011). Copper has the ability to kill the resilient spores of bacteria such as *Clostridia difficile* which causes diseases like diarrhea(Weaver, Michels et al. 2008, Wheeldon, Worthington et al. 2008). There are some possible proposed action pathways by which it is expected copper to act as an antimicrobial agent. Copper first damages the membrane of bacteria which lead to copper influx into the cells,

cause oxidative damage, fragment DNA and subsequently cell death(Warnes, Green et al. 2010, Santo, Lam et al. 2011).

Copper homeostatic system:

Some microbes like *pseudomonas aeruginosa* have genes like *CnR* encode for copper responsive regulator and CinA encode for azurin like protein which is involved in copper resistance (Elguindi, Wagner et al. 2009). Microbes like *Enterococcus hirae*has a gene called *CopB* which encodes for copper export pump. In *E.Coli* genes are present like *CueO* encodes periplasmic copper oxidase, *cus* encodes periplasmic copper efflux system and *copA* encodes cytoplasmic copper extrusion pump that are involved in copper homeostatic system (Elguindi, Wagner et al. 2009, Santo, Lam et al. 2011). The microbes with a copper resistance don't get survive from the contact killing by copper , resist to the copper system for a prolonged period of time but finally they die(Grass, Rensing et al. 2011). Non of any of bacteria completely resistant to contact killing has been found yet, because during cell death the plasmid DNAs are completely killed in cell death by this mechanism and it leaves no resistant determinants to transfer into the organisms(Warnes, Green et al. 2010). Contact killing is very rapid and it blocks the cell division on copper surface (Grass, Rensing et al. 2011).

Other possible mechanism by which copper shows antimicrobial properties is by generating ROS (Reactive oxygen species) which cause oxidative stress. ROS is produced by change in redox states between different oxidation states of copper like Cu(0), Cu(I), and Cu(II) . The absence of oxygen don't inhibit contact killing by Cu but in *E.Coli* double the time of killing(Santo, Taudte et al. 2008). Copper act as an antimicrobial agent by following different mechanism like, generation of ROS, cause oxidative damage of DNA, damage cell wall and iron sulfur containing enzymes. Cu^{2+} binds to these structures and that alter their cellular functions which ultimately leads to death of cell (Ohsumi, Kitamoto et al. 1988, Yates, Brook et al. 2008, Quaranta, Krans et al. 2011, Santo, Lam et al. 2011, Warnes and Keevil 2011).Copper interact with the sulfhydryl group of enzymes lead to formation of oxygen reactive radicals that cause protein oxidation and cleave DNA and RNA and damage the plasma membrane by lipid peroxidation (Sunada, Watanabe et al. 2003, Warnes and Keevil 2011).

As SEM analysis of feathers revealed the presence nanostructures, it is expected that various elements are involved in the formation of those nanostructures. Now a day the resistance of microbes toward antibiotics and various antimicrobial agents are increasing. Mostly there is no microbe present in both human and animal which don't show resistance to antimicrobial agent (Frye, Zweig et al. 2002). So the use of nanoparticles has given an utmost importance to fight against these microbes as well as antibiotic resistance pathogenic microbes. The antimicrobial properties of CuNP collected from different papers are shown to exhibit biocidal activity against bacteria such as *Staphylococcus aureus*(Jokar, Rahman et al. 2012), *Escherichia coli*(Zapata, Tamayo et al. 2011)*Klebsiella pneumonia*(Vimala, Mohan et al. 2010), *Pseudomonas aeruginosa*(Perkas, Amirian et al. 2007),*Enterobacter cloacae*(Kim, Lee et al. 2007), *Salmonella typhimurium* (Cárdenas,et al.,2009) and *L. monocytogenes*(Cioffi, Torsi et al. 2005).The possible mechanism of action CuNP morphological and structural changes that bring in bacterial cells , by attacking the respiratory chain and may be by forming regions of low molecular weight within the bacteria (Sondi and Salopek-Sondi 2004, Morones, Elechiguerra et al. 2005).CuNP perform antimicrobial activity by release of Cu^{2+}, that may cause the disruption of the plasmatic membrane of bacteria, enabling their entry into the bacteria and alteration of the bacteria enzymatic functions (Gunawan, Teoh et al. 2011, Xiu, Ma et al. 2011).

Chloride:

Chloride in its elemental form called chlorine, known to be the most common disinfectant, is a moderate oxidizing agent interacts with various components of cells (White 1992). The action of chlorine is proposed to damage the cell membrane of the bacterial cells (Kim, Pitts et al. 2008). Chlorine kills the microbes by disrupting the cell wall where it chlorinate the lipid protein substance present in the cell wall and form toxic chloro compounds (Venkobachar, Iyengar et al. 1977, Haas and Engelbrecht 1980). This causes the leakage of the cell wall and the macromolecules present in the cell releases out (Kim, Pitts et al. 2008).

Manganese Dioxide:

Manganese is found in the active site of many enzymes and plays an important role in the functionality of the enzyme (Larson and Pecoraro 1992). Mn forms complex by combining with various ligands and show anticancer (Li et al., 2010;Chen et al., 2010) , antibacterial

(Dorkov, Pantcheva et al. 2008) and antifungal actions (Singh et al.,2010 ; Mohamed et al., 2010). The Mn complexes react with the plasmid DNA and degrade it. Mn (II) is present as a cofactor in many enzymes. The antimicrobial activity of Mn is based on the basis of overtone concept of cell permeability. Mn element is more active in its antimicrobial properties when it is in the complex form. This increased activity of the element in its complexes can be explained on the basis of overtone and chelation theory (Islam, Farooque et al. 2002).According to overtone's concept of cell permeability the cell membrane favors the passage of only lipid soluble materials, called liposolubility is an important factor for membrane permeability that regulate antimicrobial activity on chelation with other ligand during complex formation. During chelation the polarity of metal ion is reduced to a greater extent due to overlapping of donor group of ligand orbital and partial sharing of the positive charge of the metal ion. Then this overlapping results in increases the delocalization of pi electrons over the whole ring and increases the liophilicity of the complex. The increased liophilicities of complex allow easy diffusion into lipid membranes of organisms and facilities as blockage of metal binding sites in enzyme (Gudasi, Vadavi et al. 2005).

Titanium:

Titanium in in its oxides form i.e. (TiO_2) shows antimicrobial properties and also in its nanoform (TiO_2NP) of size less than 25nm. Nanomaterials act as antimicrobial agent by hindering the action of cellular enzyme and inactivate them. Nanoparticles have ability to bind the electron donating group like carboxylate, amides, indoles, hydroxylates and thiols etc. NP penetrates the bacterial wall by forming pores on cell walls lead to increased permeability and cell death. NP act against microbes which develop resistance against the drugs. Metal oxides of NP exhibit excellent biocidal and biostatic action against gram positive and gram negative bacteria (Cuéllar-Cruz, Vega-González et al. 2012).The antimicrobial mechanism of metal oxides can be explained as the basis of charge difference that is present on the metal oxides and the charge on the microbial cells. It is proposed that the microbial cells contain negative charge and the metal oxides possess a positive charge as a result causes an electromagnetic attraction between the microorganisms and metal oxides that lead to oxidization and ultimate death of microorganisms (Li, Zhang et al. 2012). TiO2 is also involved in the formation of pigment (Baan, Straif et al. 2006). Hence it also can be proposed that it might be responsible for

exhibiting certain color in parrot. As TiO2 NP are used in sunscreen for protection against sun rays (Trouiller, Reliene et al. 2009), it also can be assumed that it might be playing some protective role in bird's feather against sun rays. TiO2 NP when exposed to nonlethal UV produce hydroxyl radicals and superoxide ions , which is shown to be highly effective in inhibiting Staphylococcus Aureus (Shah et al. 2008) and also degrade organic materials. In vivo studies show the major pathogenic mechanism initiated by TiO_2NP produce inflammatory response. The above functions of TiO_2 NP can be predicted in case of feathers of *Psitacula krameri.*

Nickel:

Nickel toxicity is given an importance as it is related with cancer in human beings (Denkhaus and Salnikow 2002, Das, Das et al. 2008). Microbes have a nickel homeostasis system to resist nickel toxicity. The exact mechanisms of nickel toxicity in microbes are unknown even though their effects on higher organisms are well demonstrated (BAEICII and Stotzky 1983). However from some of in vitro studies of nickel toxicity, some action mechanism are hypothesized like 1) nickel replaces the vital metal from metalloproteins, 2) nickel binds to catalytic sites of non-metal enzymes, 3) nickel binds the allosteric site of an enzyme to inhibit it and 4) nickel leads to oxidative stress and strain that can affect proteins, DNA, or lipids(Macomber and Hausinger 2011).

Ni-NPs have antimicrobial activity, however very few studies have done on this (Pang, Lu et al. 2009, Kumar, Rani et al. 2010). Ni-NPs shows a bacteriostatic property against *S. aureus, E. coli* and *S. mutans* (Argueta-Figueroa, Morales-Luckie et al. 2014). Other possible mechanism by which nickel act is, its ions penetrate in microbial cells and more preferably inactivate their enzymes leading to inhibit their cellular metabolic functions resulting ultimate death(Chohan 2000). Some of nickel complexes exhibit an antibacterial activity against gram positive bacteria (Popova, Smith et al. 2012). Different authors report, nickel play most of its antimicrobial properties when it is complexed with certain ligands and in other synthetic complexes.

In the collar region the presence of Ni as one of major element is expected to exhibit antimicrobial properties as discussed above, in order to keep bird free from microbial infection diseases

Tin:

Tin in its nanoparticle form in SnO_2 NP shown to have antimicrobial properties. These nano particles get adsorb on the bacterial cell and undergo dehydrogenation, due to respiration process which occurs at the cell membrane of bacteria. This reaction inactivate the bacterial enzymes by generating hydrogen peroxide that causes oxidation of bacterial cells and cause death (Awwad, Salem et al. 2012).The Because, Escherichia coli was not having cell wall it get affected more easily than *S.aureus* with cell wall (Kamaraj, Vennila et al. 2014). But the exact functions of Tin present in parrots are unknown. The above functions may be predicted.

Cobalt:

Cobalt is present in the active center of vitamin B12, (Bernhardt, Bozoglián et al. 2005) an important element found in certain cobalt-dependent proteins and in its complexes it act as hydrolytic agents for DNA cleavage (Hadjiliadis and Sletten 2009) and some have antitumor–anti-proliferative, antimicrobial, antifungal, and antiviral activity (Eshkourfu, Čobeljić et al. 2011).

Cobalt(III) in its complexes functions as an antiviral agent (Chang, Simmers et al. 2010). It is used widely in medicines for example cobalt complex CTC-96 was effective in the treatment of epithelial herpetic keratitis, identified as one of the major disease causing blindness in industrial nations (Asbellet al.,1998).The action mechanism is that CTC-96 inhibits membrane fusion events hence preventing virus entry. There by CTC-96 obstruct plaque formation by VSV (vesicular stomatitis virus) and VZV (varicella-zoster virus) (Delehanty, Bongard et al. 2008). CTC-96 also act against adenovirus (Epstein, Pashinsky et al. 2006).Co(III) in its coordination complexes act as an antibacterial agent. The possible action mechanism of these complexes can be explained on the basis of, binding to DNA of microbes to cause DNA damage (Kumar, 2008). For example some complexes like bis(ethylenediamine)cobalt(III) has screened to perform antibacterial actions against some Gram positive and Gram negative bacteria like *E. coli*, *E. coli* HB101, *Salmonella typhimurium*, *Proteus vulgaris*, *P. aeruginosa*, *S. aureus*, *S. faecalis*, *B. subtilis* (Nagababu, Latha et al. 2006).

Although the exact functions of the Cobalt and its complexes present in feather of parrots are unknown, it may be proposed they might be having antimicrobial activity against different microbes as discussed above.

Tellurium:

Tellurium very rarely found in its native state, it is found in the form of telluride of gold and in combination with other elements (Cunha, Gouvea et al. 2009).In case of parrot's feather we identified in the form of tin telluride. Already we discussed regarding the antimicrobial activity of tin. Tellurium is a metalloid and very few studies have been made on this. From these few studies it has been proposed to possess a very interesting antimicrobial activity. A novel enzyme called tellurite reductase has been purified and identified which can be used for the generation of tellurium nanostructures that has an interesting and eco-friendly antimicrobial activity which was proposed to replace AgNP or antibiotic therapy in near future (Plugin and coworkers, 2014, American Society for Microbiology,7061–7070).

Tellurium (Te) compounds have been used as antimicrobial agents in the treatment of infectious diseases (e.g., leprosy, tuberculosis, dermatitis) (Turner, Borghese et al. 2012). Recently, many synthetic organo-tellurium compounds have been developed for inhibition of bacteria growth (Daniel-Hoffmann, Sredni et al. 2012). For example, nontoxic immune modulator ammonium trichloro (dioxyethylene-O,Ó)- tellurate (AS101) is used to inhibit cysteine proteases and modulate the redox state of glutathione (Daniel-Hoffmann et al.,2012). Tellurite ($TeO_3^{2-)}$ ions have also been used to inhibit the growth of many microorganisms, particularly penicillin-resistant bacteria (Valdivia-González, Pérez-Donoso et al. 2012).The released TeO_3^{2-} ions from Te NMs have been shown effective to kill *E. coli*.31.

The mechanism of action of these Nano medicines proposed to progress through release of Te ions. Tellurium in combination with other nanostructures like Ag and Au are used in Nano medicines. The possible mechanism of action of these Nano medicines are believed to have enzyme like catalytic activity and can generate ROS (Wei and Wang 2013). However the possible biological and chemical mechanism of generation of ROS from released Te-related ions are yet to reveal (Molina-Quiroz, Muñoz-Villagrán et al. 2012, Molina-Quiroz, Loyola et al. 2013). The possible mechanism for action of ROS to inhibit bacterial growth can be explained by

following ways like through lipid peroxidation and reaction with membrane proteins, DNA, or metabolic enzymes (Lin, Shih et al. 2012).

Some other organometallic compounds of tellurium such as AS101 shown to work as an antimicrobial agent by damaging and altering the Na^+-K^+ pump on cell membrane and has been experimented in *E. cloacae.* The results showed an increase in influx of Na^+ and Cl^- destabilizes the membrane stability. The cell membrane instability was observed, shown by increase in Mg. A decrease in the level of phosphorus indicated loss of ATP and damage to DNA. It also damage cell by causing perforation in cell wall (Daniel-Hoffmann, Sredni et al. 2012).

Due to these antimicrobial properties of Tellurium it is used in drug development. The exact function of Tellurium in parrot's feathers are unknown, but keeping in view the above functions of Tellurium, the same function may be expected in bird's feathers.

Lead:

Studies have shown that long-term heavy metal contamination of soils has harmful effects on soil microbial activity, especially microbial respiration (Doelman and Haanstra 1984).Exposure of microbes to heavy metal for a long term duration alter their enzymatic activity, short term exposure reduces the microbial activity (Doelman and Haanstra 1979) .

Pb(II) toxicity occurs as a result of changes in the conformation of nucleic acids and proteins, inhibition of enzyme action, disruption of membrane functioning and oxidative phosphorylation, as well as change in osmotic balance (Bruins et al., 2000; Vallee & Ulmer,1972). Pb(II) also shows a stronger affinity for thiol and oxygen groups than essential metals such as calcium and zinc (Bruins et al., 2000). In spite of the high toxicity of Pb, many micro-organisms have developed mechanisms that facilitate them to resist and survive Pb exposure (Jarosławiecka and Piotrowska-Seget 2014).

Although the expected roles of lead in case of parrot's feather are unknown, based on the antimicrobial properties we may predict some of the above.

Zirconium:

Zirconium in its nanoparticle form that is in the form of ZrO2NP is resistant against the microbes like *Staphylococcus aureus*, *Escherichia coli* and *Pseudomonas aeruginosa (*Li and Coleman 2014*).*Zirconium in its complexes like zirconium(IV) porphyrin experimented to show antimicrobial activity against some bacterial strains, namely, *Bacillus subtilis*, *Micrococcus luteus*, *Staphylococcus aureus*, *Pseudomonas fluorescens*, and *Escherichia coli* forming zone of inhibition (Bajju, Devi et al. 2013).Very few works have been carried out regarding the antimicrobial properties of Zirconium. The exact mechanism of Zirconium antimicrobial activity is unknown and yet to reveal.

The roles of Zirconium in case of parrot's feathers are unknown, but from the few available information regarding its antimicrobial properties, the same in case of feathers may be predicted.

Silver:

Silver is an antimicrobial agent perform action in its ionic form, non-oxidative in nature. But in a cell it inactivates enzymes by binding to the –SH group (Lin et al., 1996). Silver interacts with the ribosome, inhibit the expression of enzyme and other protein responsible for ATP production (Yamanaka, Hara et al. 2005). Silver also interact with the respiratory chain and inhibit the oxidation of glucose , glycerol, fumarate (Bragg and Rainnie 1974). Silver forms a complex with DNA that is Ag-DNA complex, which is expected to cause antimicrobial activity (Arakawa, Neault et al. 2001). AgNP exhibit wide range of antimicrobial activity. AgNP gets adhered on the surface of bacteria, damage the cell wall, when the size of nanoparticle is smaller than 10nm it penetrate into bacteria (Morones, Elechiguerra et al. 2005, El Badawy, Silva et al. 2010). AgNP function as an antimicrobial agent by forming Ag+ and ROS which is the major source of toxicity (Hwang, Lee et al. 2008). Silver, may be because of its antimicrobial properties both in its ionic and complex form and hence it is expected its presence in feathers of parrot may be playing the same role.

Molybdenum:

The action of Mo as an antimicrobial agent has shown non-specific mechanism. It is believed the antimicrobial property is based on the formation of an acidic surface that inhibits cell growth

and proliferation. It is active against a broad range of both Gram positive and Gram negative bacteria, and does not produce bacterial resistance to the action of antibiotics. The acidic surface prevents the growth and proliferation of microbial cells and biofilm formation. The acidity mechanism can be explained by the diffusion of hydronium ions through the cell membrane. This results in the imbalance of pH equilibrium, which affects both enzyme proteins and the transport system of cell (Plumridge, Hesse et al. 2004). This also degrade the DNA helix (Schüller, Mamnun et al. 2004). In order to adjust this disturbed pH equilibrium mechanism energy required for the cell, that cause in further weakening of cell (Ra and Parks 2007). As the energy used against the physiological gradient. The acidic surface prevents microbes from adhering to the surface and forming bio film. But the microbes should have a direct contact with the acidic surface for antimicrobial activity (Zollfrank, Gutbrod et al. 2012).

Zinc:

In earlier studies it has been proposed that zinc play an important role in melanin synthesis in birds for imparting their feather coloration. They act upon the enzyme tyrosinase that plays a major role in the synthesis of melanin from amino acid precursors (McGraw 2003). Zinc is involved in both eumelanin and reddish brown color imparting pheomelanin synthesis (Niecke, Rothlaender et al. 2003). Zinc in its ionic, oxide and nanoparticle form has antibacterial properties (Söderberg, Sunzel et al. 1990). ZnO particles have been demonstrated to show antimicrobial properties in a wide range against both Gram positive and Gram negative bacteria like *Escherichia coli*, *Salmonella*, *Listeria monocytogenes*, and *Staphylococcus aureus* (Jones, Ray et al. 2008, Liu, He et al. 2009). The exact mechanism of antibacterial function of ZnO are exactly not cleared but, it has been proposed that it may act by disrupting cell membrane activity (Brayner, Ferrari-Iliou et al. 2006). Zinc destabilizes the cell membrane and alters by increasing the cell membrane permeability hence affect the membrane function (Stanić, Dimitrijević et al. 2010).Some other possible mechanism proposed are production of ROS (Reactive Oxygen Species), Hydrogen peroxide (H_2O_2), is a strong oxidizing agent that is harmful for bacterial cell (Sawai 2003, Jones, Ray et al. 2008). Another possible mechanism of action of Zinc has been proposed that it interacts with the nucleic acid and make the respiratory enzymes nonfunctional (Fang, Chen et al. 2006).It has been demonstrated that these oxidizing species like ROS, OH-, H_2O_2, and O_2^- are produced by UV- Visible light and those function in antimicrobial properties.

The hydroxyl radicals and super-oxides remain on the upper surface of bacterial cell whereas peroxide penetrate into the bacterial cell and induce antimicrobial properties (Padmavathy and Vijayaraghavan 2008). ZnO is used in cosmetics to protect against sunlight. It may be predicted that it might be playing some role in protecting *Psittacularis* from sunlight.

The above function of Zinc may be proposed in case of its presence in *Psittacularis* feathers. However the exact functions of its presence are unknown and more researches are required to be carried out.

Iron:

Iron plays an important role in Psittacularis feathers in imparting color. It is involved in synthesis of melanin like Zinc (McGraw 2003). Iron in forms of Porphyrin(With 1957, With 1978)and Iron Oxide (Negro, Margalida et al. 1999) can give colors to bird's feathers. The Iron nanoparticles may be involved in the antimicrobial action in bird's feather by following the mechanisms like generation of reactive oxygen species (ROS), release of harmful and toxic ions, oxidative damage through catalysis, and disturbance of the ion cell membrane transport activity by altering permeability and lipid peroxidation or surfactant properties. ROS is considered as being the main elementary chemical process in nano-toxicology which can lead to secondary processes that can ultimately cause cell damage and even cell death. Moreover, ROS is one of the main factors involved in inflammatory processes (Singh, Jenkins et al. 2010).

Hence the above functions of Iron may be expected in case of Parrot's feathers although the exact functions are unknown. However more researches need to be carried out in this field.

UV SIGNALLING IN PARROT:

Although the feather coloration is due to pigmentation and psittacofulvin, but when viewed under UV light, some portion some feathers were shown UV reflectance while not all.

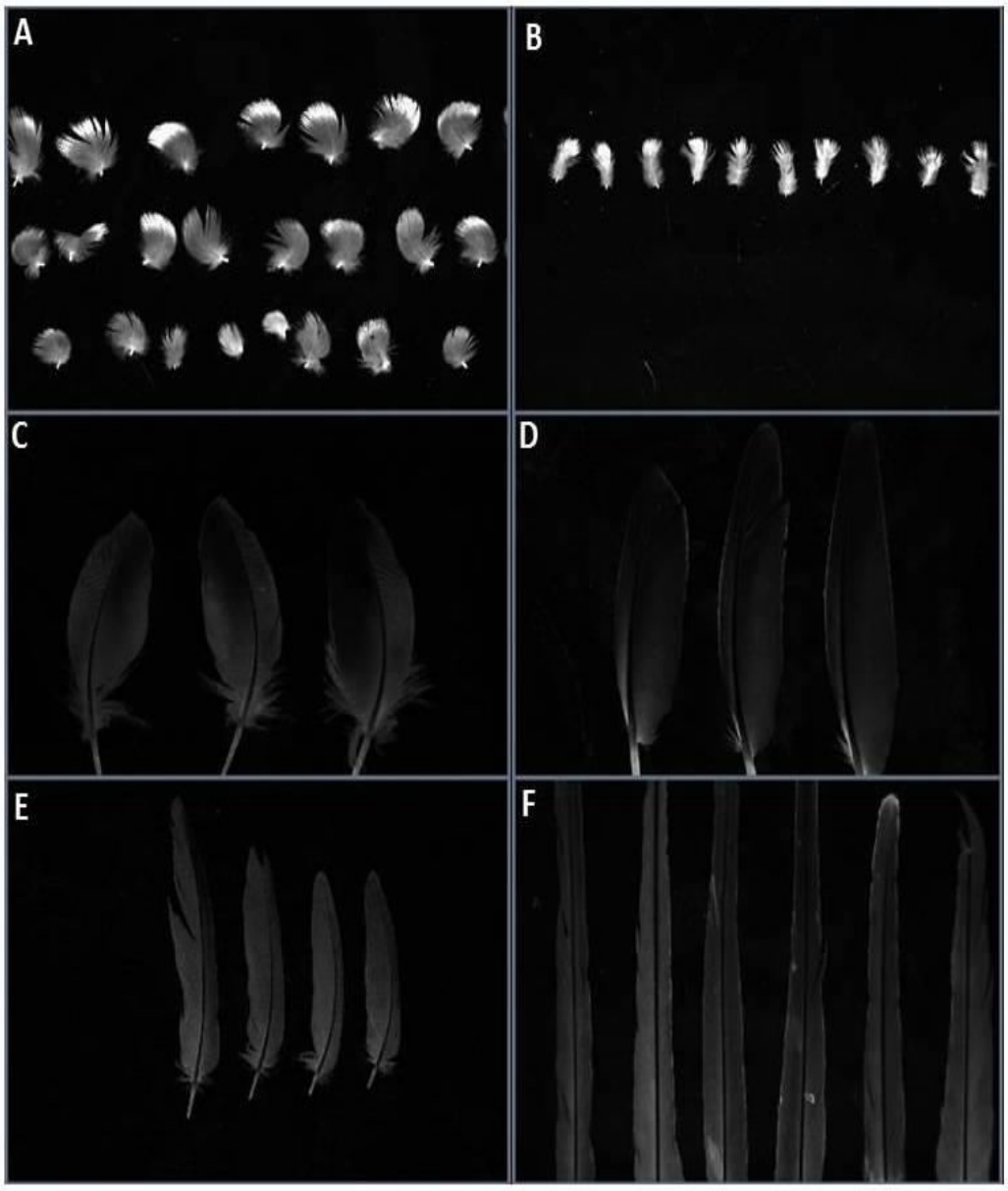

Figure 24: UV images of feathers of different part of body of Indian parrot. A- Head feather, B- Red collar of male, C- Flight feathers remiges with yellow, black and green coloration, D- Flight feathers with black and green coloration, E- Feathers of side back yellow green tail, F- Long sky blue tail.

The head feathers, flight feathers, tail feathers and collar feathers of male were viewed under UV light. Only the feathers head region, and red collar of male shown UV reflectance. The exposed tip portions of head feathers were shown UV reflectance but not the entire feather. Apart from tip portion although UV reflectance is observed in some other portions of head feather but more significant is at tip regions. In case of collar red feather of male UV reflectance was observed in the entire feather.

DISCUSSION:

SEM result discussion:

This is expected that these arrangements of the barbules are responsible for giving a structural integrity and regularity to the feathers and make it resemble as a leaf to the naked eye. It also can be proposed that this pattern of arrangement result for imparting coloration of to the feathers due to Tindall effect and reflection of light through these barbules, which is the physical basis of coloration in parrots feather or structural basis of coloration. The structural basis of coloration is produced due to the interaction between the coherent light and the nanostructures present in the feathers (Fox 1976). The structural basis of coloration can be classified into two sub-catagories called iridescent and non- iridescent. Iridescent color change in appearance when visualized through different angle and iridescent colors exhibit no change with respect to the change of geometry Newton). Both the structural colors are produced by similar coherent scattering of light by feather components but they differ by the composition and arrangement of their light scattering elements (Prum 2006). Non iridescent colors are produced due to the nanostructures present in barb. The orderly arrangement of keratin and the air in between the barbs responsible for the exhibition of non-iridescent color like blue, violet, and ultraviolet colors (Prum, Andersson et al. 2003, Shawkey, Estes et al. 2003, Doucet, Shawkey et al. 2004), Iridescent colors produced due to the structure and arrangement of barbules (Prum 2006). In case of barbules the constructive scattering of coherent light takes place between keratin, melanin and air present alternatively with a variable refractive index (Doucet, Mennill et al. 2005). The variation in the nanostructures that are present in barbules responsible for various colors .It also can be proposed that this interlocking pattern of arrangement of the barbules help the bird to prevent water flow to reach its body surface hence making feathers impermeable to water. This

may prevent the bird to get less affected during rain, and also get rid of microbial infections up to some extent. This interlocking pattern of arrangement of barbules also can be responsible for making the feathers more insulated by closing the air spaces on it which again prevent the bird from cold.

In each feathers we obtained different measurements for different structural components. The shape and different components and their arrangement also vary from feather to feather. This variations may result in exhibiting the phenomena of iridescent of light. This is the reason why one can observe various color when observed through different angles. The same is observed in case of feathers of parrots due to its different structural build up as well as arrangement of various components. The tail feathers are expected to show iridescent coloration in a higher degree.

Though in some cases we observed some similarities in their structural components like barbs, barbules and their arrangement, but the structures and arrangement of the terminal end of barbules varies. It is expected this variations in structural buildup of barbules are responsible for exhibiting the phenomena of refraction , Tindall effect as well as scattering of light, as in a same feather we observed various length , structures and arrangement of barbule terminals.

XRD result discussion:

The elements obtained from the XRD data analysis are predicted to play an antimicrobial activity or play role in coloration of feathers. These elements both in their ionic form as well as in their complexes may be playing both of the roles. Some transition elements are also obtained in XRD peaks like Cobalt, Nickel, and Manganese etc., which have a chemical property of forming coordination complexes with some ligands. An important property of these coordinating complexes are to show color , which may be contributing for color exhibition in feathers up to some extent, although the primary factors of color formation are pigmentation and Tindall effect ,the physical basis of color formation. Very few works have been carried out in this field so the microbial action mechanism of many elements is unknown. The exact role of these elements and their complexes in feathers are some of questions need to be answered.

Discussion of UV result:

It has been reported some microstructures are present in barb (Fox 1976, Prum, Andersson et al. 2003) of some feathers responsible for UV reflectance, along with the blue violet and other iridescent colors (Korsten, Vedder et al. 2007). It has been found that feathers of many bird species show UV reflectance (Burkhardt 1989, Eaton and Lanyon 2003), many species have the ability to detect the UV region of spectrum (Parrish, Ptacek et al. 1984, Cuthill, Partridge et al. 2000), which normal human eye can't do. Several studies have shown that UV reflectance play a major role in mate selection. Female give preference to high UV reflectance male species than low reflectance (Andersson and Andersson 1998, Johnsen, Andersson et al. 1998).

UV reflectance may be a good medium of social signaling for mate selection because of its short wavelength for which it can be a signaling medium over shorter distance and it may be distorted over longer distance due to scattering by particles (Lythgoe 1979, Andersson 1996). Some authors has been suggested that UV may be a secret avian communication channel which many potential mammals cannot read (Guilford and Harvey 1998). As chlorophyll absorbs UV light, plants may provide a contrasting background to UV reflective feathers which may make UV a good signaling medium in avian community (Andersson and Andersson 1998). It has been suggested that bird's feather are sensitive to UV wavelength than other wavelength (Burkhardt and Maier 1989), may be because of their sensitive vision toward UV wavelength to which they are pre-exposed which may help them to search their food (Church, Bennett et al. 1998). UV signals are iridescent which may help bird's to help in their courtship selection with an accuracy and greater potency.

Conclusion:

Very few experiments are conducted about Indian parrot. Depending upon the information that are present about feathers of other birds we tried to propose some information regarding the nanostructures present in feathers and their role in coloration in parrot. By observing the different structures and arrangement of barbules the expected function of barbules were proposed to involve in iridescent and non-iridescent coloration. The SEM imaging magnified the various feather components out of their nanostructure form. However these varied structures and pattern formation of these feather components are expected to responsible for the different color

exhibition by different feathers. This is expected because, although to naked eye these feather components almost seems similar to each other but their SEM imaging structures particularly the structure and arrangement of barbules to pattern formation are different from each other as observed from all those images. From the XRD analysis data the elements present in the feather microstructures were detected. Although the exact functions of these elements in parrot's feather are unknown, some of the antimicrobial properties of them were expected. The elements detected from the XRD predicted to present in its nano form and might be playing many more roles. The element detection reveals many elements which are present in nature and are not studied yet. In order to study those, the laboratory synthesis is required. The study of these structures in laboratory may discover some other amazing dimensions of these elements in their nano form. From UV imaging of the various feathers the function was predicted to be helpful in courtship or mate selection or in social signaling. The red collar feathers of the male shows UV reflectance which may be helpful for female for male selection. The UV reflectance of other feathers like head feather may be helpful in potent male selection. The phenomenon of scattering of coherent light was discussed in order to understand iridescent and non -iridescent coloration and pigmentation. However further researches are required to unravel the story behind this phenomenal feather coloration of nature.

REFERENCES:

Auber, L. (1957). THE STRUCTURES PRODUCING "NON- IRIDESCENT" BLUE COLOUR IN BIRD FEATHERS. Proceedings of the Zoological Society of London, Wiley Online Library.

Brush, A. H. (1990). "Metabolism of carotenoid pigments in birds." The FASEB Journal**4**(12): 2969-2977.

Burkhardt, D. (1989). "UV vision: a bird's eye view of feathers." Journal of Comparative Physiology A**164**(6): 787-796.

Cuthill, I. C., et al. (2000). "Ultraviolet vision in birds." Advances in the Study of Behavior**29**: 159-214.

Eaton, M. D. and S. M. Lanyon (2003). "The ubiquity of avian ultraviolet plumage reflectance." Proceedings of the Royal Society of London. Series B: Biological Sciences**270**(1525): 1721-1726.

Fox, D. L. (1976). Animal Biochromes and Structural Colours: Physical, Chemical, Distribution & Physiological Features of Coloured Bodies in the Animal World, University of California Press.

Hausmann, F., et al. (2003). "Ultraviolet signals in birds are special." Proceedings of the Royal Society of London B: Biological Sciences**270**(1510): 61-67.

Hill, G. E. (1999). "Is There an Immunological Cost to Carotenoid- Based Ornamental Coloration?" The American Naturalist**154**(5): 589-595.

Hill, G. E. (2000). "Energetic constraints on expression of carotenoidâ€• based plumage coloration." Journal of Avian Biology**31**(4): 559-566.

Hill, G. E., et al. (2002). "Dietary carotenoids predict plumage coloration in wild house finches." Proceedings of the Royal Society of London B: Biological Sciences**269**(1496): 1119-1124.

Jawor, J. M. and R. Breitwisch (2003). "Melanin ornaments, honesty, and sexual selection." The Auk**120**(2): 249-265.

M Hofmann, C., et al. (2007). "Melanin coloration in New World orioles I: carotenoid masking and pigment dichromatism in the orchard oriole complex." Journal of Avian Biology**38**(2): 163-171.

McGraw, K. J., et al. (2004). "European barn swallows use melanin pigments to color their feathers brown." Behavioral Ecology**15**(5): 889-891.

Olson, V. r. A. and I. P. F. Owens (1998). "Costly sexual signals: are carotenoids rare, risky or required?" Trends in Ecology & Evolution**13**(12): 510-514.

Parrish, J. W., et al. (1984). "The detection of near-ultraviolet light by nonmigratory and migratory birds." The Auk: 53-58.

Prum, R. O., et al. (2003). "Coherent scattering of ultraviolet light by avian feather barbs." The Auk**120**(1): 163-170.

Andersson, S. (1996). "Bright ultraviolet colouration in the Asian whistling-thrushes (Myiophonus spp.)." Proceedings of the Royal Society of London. Series B: Biological Sciences **263**(1372): 843-848.

Andersson, S. and M. Andersson (1998). "Ultraviolet sexual dimorphism and assortative mating in blue tits." Proceedings of the Royal Society of London. Series B: Biological Sciences **265**(1395): 445-450.

Arakawa, H., et al. (2001). "Silver (I) complexes with DNA and RNA studied by Fourier transform infrared spectroscopy and capillary electrophoresis." Biophysical Journal **81**(3): 1580-1587.

Argueta-Figueroa, L., et al. (2014). "Synthesis, characterization and antibacterial activity of copper, nickel and bimetallic Cu–Ni nanoparticles for potential use in dental materials." Progress in Natural Science: Materials International **24**(4): 321-328.

Auber, L. (1957). THE STRUCTURES PRODUCING "NON- IRIDESCENT" BLUE COLOUR IN BIRD FEATHERS. Proceedings of the Zoological Society of London, Wiley Online Library.

Awwad, A. M., et al. (2012). "Biosynthesis of silver nanoparticles using Olea europaea leaves extract and its antibacterial activity." Nanoscience and Nanotechnology **2**(6): 164-170.

Baan, R., et al. (2006). "Carcinogenicity of carbon black, titanium dioxide, and talc." The lancet oncology **7**(4): 295-296.

BAEICII, H. and G. Stotzky (1983). "Toxicity of nickel to microbes: environmental aspects." Advances in applied microbiology **29**: 195.

Bajju, G. D., et al. (2013). "Synthesis, spectroscopic, and biological studies on new zirconium (IV) porphyrins with axial ligand." Bioinorganic chemistry and applications **2013**.

Bernhardt, P. V., et al. (2005). "Molecular mixed-valence cyanide bridged Co III–Fe II complexes." Coordination chemistry reviews **249**(17): 1902-1916.

Bragg, P. and D. Rainnie (1974). "The effect of silver ions on the respiratory chain of Escherichia coli." Canadian journal of microbiology **20**(6): 883-889.

Brayner, R., et al. (2006). "Toxicological impact studies based on Escherichia coli bacteria in ultrafine ZnO nanoparticles colloidal medium." Nano Letters **6**(4): 866-870.

Brush, A. H. (1990). "Metabolism of carotenoid pigments in birds." The FASEB Journal **4**(12): 2969-2977.

Burkhardt, D. (1989). "UV vision: a bird's eye view of feathers." Journal of Comparative Physiology A **164**(6): 787-796.

Burkhardt, D. and E. Maier (1989). "The spectral sensitivity of a passerine bird is highest in the UV." Naturwissenschaften **76**(2): 82-83.

Chang, E. L., et al. (2010). "Cobalt complexes as antiviral and antibacterial agents." Pharmaceuticals **3**(6): 1711-1728.

Chohan, Z. H. (2000). "SYMMETRIC 1, 1-DIMETHYLFERROCENE-DERIVED AMINO ACIDS: THEIR SYNTHESIS, CHARACTERIZATION, LIGATIONAL AND BIOLOGICAL PROPERTIES WITH Cu (II), Co (II) and Ni (II) IONS." Metal Based Drugs **7**: 177-184.

Church, S. C., et al. (1998). "Ultraviolet cues affect the foraging behaviour of blue tits." Proceedings of the Royal Society of London. Series B: Biological Sciences **265**(1405): 1509-1514.

Cioffi, N., et al. (2005). "Copper nanoparticle/polymer composites with antifungal and bacteriostatic properties." Chemistry of Materials **17**(21): 5255-5262.

Cuéllar-Cruz, M., et al. (2012). "The effect of biomaterials and antifungals on biofilm formation by Candida species: a review." European journal of clinical microbiology & infectious diseases **31**(10): 2513-2527.

Cunha, R. L., et al. (2009). "A glimpse on biological activities of tellurium compounds." Anais da Academia Brasileira de Ciências **81**(3): 393-407.

Cuthill, I. C., et al. (2000). "Ultraviolet vision in birds." Advances in the Study of Behavior **29**: 159-214.

Cuthill, I. C., et al. (2000). "Ultraviolet vision in birds." Advances in the Study of Behavior **29**: 159-214.

Daniel-Hoffmann, M., et al. (2012). "Bactericidal activity of the organo-tellurium compound AS101 against Enterobacter cloacae." Journal of Antimicrobial Chemotherapy: dks185.

Das, K., et al. (2008). "Nickel, its adverse health effects & oxidative stress." Indian Journal of Medical Research **128**(4): 412.

Delehanty, J. B., et al. (2008). "Antiviral properties of cobalt (III)-complexes." Bioorganic & medicinal chemistry **16**(2): 830-837.

Denkhaus, E. and K. Salnikow (2002). "Nickel essentiality, toxicity, and carcinogenicity." Critical reviews in oncology/hematology **42**(1): 35-56.

Doelman, P. and L. Haanstra (1979). "Effects of lead on the soil bacterial microflora." Soil Biology and Biochemistry **11**(5): 487-491.

Doelman, P. and L. Haanstra (1984). "Short-term and long-term effects of cadmium, chromium, copper, nickel, lead and zinc on soil microbial respiration in relation to abiotic soil factors." Plant and soil **79**(3): 317-327.

Dollwet, H. and J. Sorenson (1985). "Historic uses of copper compounds in medicine." Trace elements in Medicine **2**(2): 80-87.

Dorkov, P., et al. (2008). "Synthesis, structure and antimicrobial activity of manganese (II) and cobalt (II) complexes of the polyether ionophore antibiotic Sodium Monensin A." Journal of inorganic biochemistry **102**(1): 26-32.

Doucet, S., et al. (2004). "Concordant evolution of plumage colour, feather microstructure and a melanocortin receptor gene between mainland and island populations of a fairy–wren." Proceedings of the Royal Society of London B: Biological Sciences **271**(1549): 1663-1670.

Doucet, S. M., et al. (2005). "Achromatic plumage reflectance predicts reproductive success in male black-capped chickadees." Behavioral Ecology **16**(1): 218-222.

DYCK, J. (1985). "The Evolution of Feathers*." Zoologica Scripta **14**(2): 137-154.

Eaton, M. D. and S. M. Lanyon (2003). "The ubiquity of avian ultraviolet plumage reflectance." Proceedings of the Royal Society of London. Series B: Biological Sciences **270**(1525): 1721-1726.

El Badawy, A. M., et al. (2010). "Surface charge-dependent toxicity of silver nanoparticles." Environmental science & technology **45**(1): 283-287.

Elguindi, J., et al. (2009). "Genes involved in copper resistance influence survival of Pseudomonas aeruginosa on copper surfaces." Journal of Applied Microbiology **106**(5): 1448-1455.

Eliason, C. M. and M. D. Shawkey (2012). "A photonic heterostructure produces diverse iridescent colours in duck wing patches." Journal of The Royal Society Interface **9**(74): 2279-2289.

Epstein, S. P., et al. (2006). "Efficacy of topical cobalt chelate CTC-96 against adenovirus in a cell culture model and against adenovirus keratoconjunctivitis in a rabbit model." BMC ophthalmology **6**(1): 22.

Eshkourfu, R., et al. (2011). "Synthesis, characterization, cytotoxic activity and DNA binding properties of the novel dinuclear cobalt (III) complex with the condensation product of 2-acetylpyridine and malonic acid dihydrazide." Journal of inorganic biochemistry **105**(9): 1196-1203.

Faivre, B., et al. (2003). "Immune activation rapidly mirrored in a secondary sexual trait." Science **300**(5616): 103-103.

Fang, M., et al. (2006). "Antibacterial activities of inorganic agents on six bacteria associated with oral infections by two susceptibility tests." International Journal of Antimicrobial Agents **27**(6): 513-517.

Fox, D. L. (1976). Animal Biochromes and Structural Colours: Physical, Chemical, Distribution & Physiological Features of Coloured Bodies in the Animal World, University of California Press.

Frye, D. M., et al. (2002). "An outbreak of febrile gastroenteritis associated with delicatessen meat contaminated with Listeria monocytogenes." Clinical infectious diseases **35**(8): 943-949.

Grass, G., et al. (2011). "Metallic copper as an antimicrobial surface." Applied and environmental microbiology **77**(5): 1541-1547.

Grether, G. F., et al. (2005). "Carotenoid availability affects the development of a colour-based mate preference and the sensory bias to which it is genetically linked." Proceedings of the Royal Society B: Biological Sciences **272**(1577): 2181-2188.

Gudasi, K. B., et al. (2005). "Five-coordinate cobalt (II), nickel (II) and zinc (II) complexes derived from 2-pyridine-2-yl-3-(pyridine-2-carboxylideneamino)-1, 2-dihydroquinazolin-4 (3H)-one. The crystal structure of the cobalt (II) complex." Transition metal chemistry **30**(6): 661-668.

Guilford, T. and P. H. Harvey (1998). "Ornithology: The purple patch." Nature **392**(6679): 867-869.

Gunawan, C., et al. (2011). "Cytotoxic origin of copper (II) oxide nanoparticles: comparative studies with micron-sized particles, leachate, and metal salts." ACS nano **5**(9): 7214-7225.

Haas, C. N. and R. S. Engelbrecht (1980). "Physiological alterations of vegetative microorganisms resulting form chlorination." Journal (Water Pollution Control Federation): 1976-1989.

Hadjiliadis, N. D. and E. Sletten (2009). Metal complex-DNA interactions, Wiley Online Library.

Hausmann, F., et al. (2003). "Ultraviolet signals in birds are special." Proceedings of the Royal Society of London B: Biological Sciences **270**(1510): 61-67.

Hill, G. E. (1999). "Is There an Immunological Cost to Carotenoid- Based Ornamental Coloration?" The American Naturalist **154**(5): 589-595.

Hill, G. E. (2000). "Energetic constraints on expression of carotenoidâ€• based plumage coloration." Journal of Avian Biology **31**(4): 559-566.

Hill, G. E., et al. (2002). "Dietary carotenoids predict plumage coloration in wild house finches." Proceedings of the Royal Society of London B: Biological Sciences **269**(1496): 1119-1124.

Hill, G. E. and K. J. McGraw (2006). Bird coloration: mechanisms and measurements, Harvard University Press.

Hudon, J. and A. H. Brush (1992). "[29] Identification of carotenoid pigments in birds." Methods in Enzymology **213**: 312-321.

Hwang, E. T., et al. (2008). "Analysis of the Toxic Mode of Action of Silver Nanoparticles Using Stress- Specific Bioluminescent Bacteria." Small **4**(6): 746-750.

Islam, M. S., et al. (2002). "Antimicrobial and toxicological studies of mixed ligand transition metal complexes of Schiff bases." OnLine Journal of Biological Sciences (Pakistan).

Jarosławiecka, A. and Z. Piotrowska-Seget (2014). "Lead resistance in micro-organisms." Microbiology **160**(Pt 1): 12-25.

Jawor, J. M. and R. Breitwisch (2003). "Melanin ornaments, honesty, and sexual selection." The Auk **120**(2): 249-265.

Johnsen, A., et al. (1998). "Ultraviolet plumage ornamentation affects social mate choice and sperm competition in bluethroats (Aves: Luscinia s. svecica): a field experiment." Proceedings of the Royal Society of London. Series B: Biological Sciences **265**(1403): 1313-1318.

Jokar, M., et al. (2012). "Melt production and antimicrobial efficiency of low-density polyethylene (LDPE)-silver nanocomposite film." Food and bioprocess technology **5**(2): 719-728.

Jones, N., et al. (2008). "Antibacterial activity of ZnO nanoparticle suspensions on a broad spectrum of microorganisms." FEMS microbiology letters **279**(1): 71-76.

Kamaraj, P., et al. (2014). "BIOLOGICAL ACTIVITIES OF TIN OXIDE NANOPARTICLES SYNTHESIZED USING PLANT EXTRACT."

Kim, J., et al. (2008). "Comparison of the antimicrobial effects of chlorine, silver ion, and tobramycin on biofilm." Antimicrobial agents and chemotherapy **52**(4): 1446-1453.

Kim, Y. H., et al. (2007). "Synthesis and characterization of antibacterial Ag-SiO2 nanocomposite." The Journal of Physical Chemistry C **111**(9): 3629-3635.

Korsten, P., et al. (2007). "Absence of status signalling by structurally based ultraviolet plumage in wintering blue tits (Cyanistes caeruleus)." Behavioral Ecology and Sociobiology **61**(12): 1933-1943.

Kumar, H., et al. (2010). "Reverse micellar synthesis, characterization & antibacterial study of nickel nanoparticles." Advances in Control, Chemical Engineering, Civil Engineering and Mechanical Engineering: 88-94.

Larson, E. and V. Pecoraro (1992). "Introduction to manganese enzymes." Manganese Redox Enzymes: 1-28.

Li, Q. and N. J. Coleman (2014). "Hydration kinetics, ion-release and antimicrobial properties of white Portland cement blended with zirconium oxide nanoparticles." Dental materials journal **33**(6): 805-810.

Li, Y., et al. (2012). "Mechanism of photogenerated reactive oxygen species and correlation with the antibacterial properties of engineered metal-oxide nanoparticles." ACS nano **6**(6): 5164-5173.

Lin, Z. H., et al. (2012). "Preparation of photocatalytic Au–Ag2Te nanomaterials." Chemistry-A European Journal **18**(39): 12330-12336.

Liu, Y., et al. (2009). "Antibacterial activities of zinc oxide nanoparticles against Escherichia coli O157: H7." Journal of Applied Microbiology **107**(4): 1193-1201.

Lucas, A. and P. Stettenheim (1972). "Avian Anatomy-Integument. Agricultural Handbook. 362: Agricultural Research Services." US Department of Agriculture, Washington, DC.

Lythgoe, J. N. (1979). Ecology of vision, Clarendon Press; Oxford University Press.

M Hofmann, C., et al. (2007). "Melanin coloration in New World orioles I: carotenoid masking and pigment dichromatism in the orchard oriole complex." Journal of Avian Biology **38**(2): 163-171.

Macomber, L. and R. P. Hausinger (2011). "Mechanisms of nickel toxicity in microorganisms." Metallomics **3**(11): 1153-1162.

Maia, R., et al. (2012). "Social environment affects acquisition and color of structural nuptial plumage in a sexually dimorphic tropical passerine." PloS one **7**(10): e47501.

McGraw, K. and M. Nogare (2004). "Carotenoid pigments and the selectivity of psittacofulvin-based coloration systems in parrots." Comparative Biochemistry and Physiology Part B: Biochemistry and Molecular Biology **138**(3): 229-233.

McGraw, K. J. (2003). "Melanins, metals, and mate quality." Oikos: 402-406.

McGraw, K. J. (2005). "The antioxidant function of many animal pigments: are there consistent health benefits of sexually selected colourants?" Animal Behaviour **69**(4): 757-764.

McGraw, K. J., et al. (2004). "European barn swallows use melanin pigments to color their feathers brown." Behavioral Ecology **15**(5): 889-891.

Molina-Quiroz, R. C., et al. (2013). "DNA, cell wall and general oxidative damage underlie the tellurite/cefotaxime synergistic effect in Escherichia coli." PloS one **8**(11): e79499.

Molina-Quiroz, R. C., et al. (2012). "Enhancing the antibiotic antibacterial effect by sub lethal tellurite concentrations: tellurite and cefotaxime act synergistically in Escherichia coli." PloS one **7**(4): e35452.

Morones, J. R., et al. (2005). "The bactericidal effect of silver nanoparticles." Nanotechnology **16**(10): 2346.

Nagababu, P., et al. (2006). "Studies on antimicrobial activity of cobalt (III) ethylenediamine complexes." Canadian journal of microbiology **52**(12): 1247-1254.

Negro, J. J., et al. (1999). "The function of the cosmetic coloration of bearded vultures: when art imitates life." Animal Behaviour **58**(5): F14-F17.

Nemésio, A. (2001). "Colour production and evolution in parrots." Int. J. Ornithol **4**: 75-102.

Newton, I. Dover Publications; Mineola, NY: 1704, Opticks.

Newton, I. (1952). "1730." Opticks, or a Treatise of the Reflections, Refractions, Inflections and Colours of Light: 378.

Niecke, M., et al. (2003). "Why do melanin ornaments signal individual quality? Insights from metal element analysis of barn owl feathers." Oecologia **137**(1): 153-158.

Ohsumi, Y., et al. (1988). "Changes induced in the permeability barrier of the yeast plasma membrane by cupric ion." Journal of Bacteriology **170**(6): 2676-2682.

Olson, V. r. A. and I. P. F. Owens (1998). "Costly sexual signals: are carotenoids rare, risky or required?" Trends in Ecology & Evolution **13**(12): 510-514.

Padmavathy, N. and R. Vijayaraghavan (2008). "Enhanced bioactivity of ZnO nanoparticles—an antimicrobial study." Science and Technology of Advanced Materials **9**(3): 035004.

Pang, H., et al. (2009). "Facile synthesis of nickel oxide nanotubes and their antibacterial, electrochemical and magnetic properties." Chem. Commun.(48): 7542-7544.

Parrish, J. W., et al. (1984). "The detection of near-ultraviolet light by nonmigratory and migratory birds." The Auk: 53-58.

Perkas, N., et al. (2007). "Ultrasound- assisted coating of nylon 6, 6 with silver nanoparticles and its antibacterial activity." Journal of applied polymer science **104**(3): 1423-1430.

Plumridge, A., et al. (2004). "The weak acid preservative sorbic acid inhibits conidial germination and mycelial growth of Aspergillus niger through intracellular acidification." Applied and environmental microbiology **70**(6): 3506-3511.

Popova, L., et al. (2012). "Immunodominance of antigenic site B over site A of hemagglutinin of recent H3N2 influenza viruses." PloS one **7**(7): e41895.

Prum, R. (2006). Anatomy, physics, and evolution of avian structural colors. Á In: Hill, GE and McGraw, KJ (eds). Bird coloration, volume 1: mechanisms and measurements, Harvard University Press, Cambridge, pp. 295Á355.

Prum, R. O. (2006). "Anatomy, physics, and evolution of structural colors." Bird coloration **1**: 295-353.

Prum, R. O., et al. (2003). "Coherent scattering of ultraviolet light by avian feather barbs." The Auk **120**(1): 163-170.

Quaranta, D., et al. (2011). "Mechanisms of contact-mediated killing of yeast cells on dry metallic copper surfaces." Applied and environmental microbiology **77**(2): 416-426.

Ra, H.-J. and W. C. Parks (2007). "Control of matrix metalloproteinase catalytic activity." Matrix biology **26**(8): 587-596.

Ralph, C. L. (1969). "The control of color in birds." American Zoologist **9**(2): 521-530.

Santo, C. E., et al. (2011). "Bacterial killing by dry metallic copper surfaces." Applied and environmental microbiology **77**(3): 794-802.

Santo, C. E., et al. (2008). "Contribution of copper ion resistance to survival of Escherichia coli on metallic copper surfaces." Applied and environmental microbiology **74**(4): 977-986.

Sawai, J. (2003). "Quantitative evaluation of antibacterial activities of metallic oxide powders (ZnO, MgO and CaO) by conductimetric assay." Journal of Microbiological Methods **54**(2): 177-182.

Schüller, C., et al. (2004). "Global phenotypic analysis and transcriptional profiling defines the weak acid stress response regulon in Saccharomyces cerevisiae." Molecular biology of the cell **15**(2): 706-720.

Shawkey, M. D., et al. (2003). "Nanostructure predicts intraspecific variation in ultraviolet–blue plumage colour." Proceedings of the Royal Society of London B: Biological Sciences **270**(1523): 1455-1460.

Singh, N., et al. (2010). "Potential toxicity of superparamagnetic iron oxide nanoparticles (SPION)." Nano reviews **1**.

Söderberg, T. A., et al. (1990). "Antibacterial effect of zinc oxide in vitro." Scandinavian Journal of Plastic and Reconstructive Surgery and Hand Surgery **24**(3): 193-197.

Sondi, I. and B. Salopek-Sondi (2004). "Silver nanoparticles as antimicrobial agent: a case study on E. coli as a model for Gram-negative bacteria." Journal of colloid and interface science **275**(1): 177-182.

Stanić, V., et al. (2010). "Synthesis, characterization and antimicrobial activity of copper and zinc-doped hydroxyapatite nanopowders." Applied Surface Science **256**(20): 6083-6089.

Stradi, R. (1998). The colour of flight: carotenoids in bird plumage, Solei Gruppo Editoriale Informatico.

Stradi, R., et al. (2001). "The chemical structure of the pigments in Ara macao plumage." Comparative Biochemistry and Physiology Part B: Biochemistry and Molecular Biology **130**(1): 57-63.

Sunada, K., et al. (2003). "Bactericidal activity of copper-deposited TiO2 thin film under weak UV light illumination." Environmental science & technology **37**(20): 4785-4789.

Torquato, S., et al. (2000). "Is random close packing of spheres well defined?" Physical review letters **84**(10): 2064.

Trouiller, B., et al. (2009). "Titanium dioxide nanoparticles induce DNA damage and genetic instability in vivo in mice." Cancer research **69**(22): 8784-8789.

Turner, R. J., et al. (2012). "Microbial processing of tellurium as a tool in biotechnology." Biotechnology advances **30**(5): 954-963.

Valdivia-González, M., et al. (2012). "Effect of tellurite-mediated oxidative stress on the Escherichia coli glycolytic pathway." Biometals **25**(2): 451-458.

Venkobachar, C., et al. (1977). "Mechanism of disinfection: effect of chlorine on cell membrane functions." Water Research **11**(8): 727-729.

Veronelli, M., et al. (1995). "In situ resonance Raman spectra of carotenoids in bird's feathers." Journal of Raman Spectroscopy **26**(8- 9): 683-692.

Vimala, K., et al. (2010). "Fabrication of porous chitosan films impregnated with silver nanoparticles: a facile approach for superior antibacterial application." Colloids and Surfaces B: Biointerfaces **76**(1): 248-258.

Warnes, S., et al. (2010). "Biocidal efficacy of copper alloys against pathogenic enterococci involves degradation of genomic and plasmid DNAs." Applied and environmental microbiology **76**(16): 5390-5401.

Warnes, S. and C. Keevil (2011). "Mechanism of copper surface toxicity in vancomycin-resistant enterococci following wet or dry surface contact." Applied and environmental microbiology **77**(17): 6049-6059.

Weaver, L., et al. (2008). "Survival of Clostridium difficile on copper and steel: futuristic options for hospital hygiene." Journal of Hospital Infection **68**(2): 145-151.

Wei, H. and E. Wang (2013). "Nanomaterials with enzyme-like characteristics (nanozymes): next-generation artificial enzymes." Chemical Society Reviews **42**(14): 6060-6093.

Wheeldon, L., et al. (2008). "Antimicrobial efficacy of copper surfaces against spores and vegetative cells of Clostridium difficile: the germination theory." Journal of Antimicrobial Chemotherapy **62**(3): 522-525.

Wilts, B. D., et al. (2012). "Brilliant camouflage: photonic crystals in the diamond weevil, Entimus imperialis." Proceedings of the Royal Society B: Biological Sciences: rspb20112651.

With, T. (1957). "Pure Unequivocal Uroporphyrin III Simplified Method of Preparation from Turaco Feathers." Scandinavian Journal of Clinical & Laboratory Investigation **9**(4): 398-401.

With, T. K. (1978). "On porphyrins in feathers of owls and bustards." International Journal of Biochemistry **9**(12): 893-895.

Xiu, Z.-M., et al. (2011). "Differential effect of common ligands and molecular oxygen on antimicrobial activity of silver nanoparticles versus silver ions." Environmental science & technology **45**(20): 9003-9008.

Yamanaka, M., et al. (2005). "Bactericidal actions of a silver ion solution on Escherichia coli, studied by energy-filtering transmission electron microscopy and proteomic analysis." Applied and environmental microbiology **71**(11): 7589-7593.

Yates, H., et al. (2008). "Photo-induced self-cleaning and biocidal behaviour of titania and copper oxide multilayers." Journal of Photochemistry and Photobiology A: Chemistry **197**(2): 197-205.

Yoshioka, S. and S. Kinoshita (2002). "Effect of macroscopic structure in iridescent color of the peacock feathers." FORMA-TOKYO- **17**(2): 169-181.

Zapata, P. A., et al. (2011). "Nanocomposites based on polyethylene and nanosilver particles produced by metallocenic “in situ” polymerization: synthesis, characterization, and antimicrobial behavior." European Polymer Journal **47**(8): 1541-1549.

Zollfrank, C., et al. (2012). "Antimicrobial activity of transition metal acid MoO 3 prevents microbial growth on material surfaces." Materials Science and Engineering: C **32**(1): 47-54.